The Plant Cell, Vol. 24: 5106–5122, December 2012, www.plantcell.org

UBIQUITIN-SPECIFIC PROTEASE16 Modulates Salt Tolerance in *Arabidopsis* by Regulating Na^+/H^+ Antiport Activity and Serine Hydroxymethyltransferase Stability[C][W]

Huapeng Zhou,[a,b,c,1] Jinfeng Zhao,[d,1] Yongqing Yang,[c] Changxi Chen,[c] Yanfen Liu,[b] Xuehua Jin,[c] Limei Chen,[c] Xueyong Li,[d] Xing Wang Deng,[e] Karen S. Schumaker,[f] and Yan Guo[c,2]

[a] College of Life Science, Beijing Normal University, Beijing 100875, China
[b] National Institute of Biological Sciences, Beijing 102206, China
[c] State Key Laboratory of Plant Physiology and Biochemistry, College of Biological Sciences, China Agricultural University, Beijing 100193, China
[d] National Key Facility for Crop Gene Resources and Genetic Improvement, Institute of Crop Science, Chinese Academy of Agriculture Sciences, Beijing 100081, China
[e] Department of Molecular, Cellular, and Developmental Biology, Yale University, New Haven, Connecticut 06520
[f] School of Plant Sciences, University of Arizona, Tucson, Arizona 85721

Protein ubiquitination is a reversible process catalyzed by ubiquitin ligases and ubiquitin-specific proteases (UBPs). We report the identification and characterization of UBP16 in *Arabidopsis thaliana*. UBP16 is a functional ubiquitin-specific protease and its enzyme activity is required for salt tolerance. Plants lacking UBP16 were hypersensitive to salt stress and accumulated more sodium and less potassium. UBP16 positively regulated plasma membrane Na^+/H^+ antiport activity. Through yeast two-hybrid screening, we identified a putative target of UBP16, SERINE HYDROXYMETHYLTRANSFERASE1 (SHM1), which has previously been reported to be involved in photorespiration and salt tolerance in *Arabidopsis*. We found that SHM1 is degraded in a 26S proteasome–dependent process, and UBP16 stabilizes SHM1 by removing the conjugated ubiquitin. Ser hydroxymethyltransferase activity is lower in the *ubp16* mutant than in the wild type but higher than in the *shm1* mutant. During salt stress, UBP16 and SHM1 function in preventing cell death and reducing reactive oxygen species accumulation, activities that are correlated with increasing Na^+/H^+ antiport activity. Overexpression of SHM1 in the *ubp16* mutant partially rescues its salt-sensitive phenotype. Taken together, our results suggest that UBP16 is involved in salt tolerance in *Arabidopsis* by modulating sodium transport activity and repressing cell death at least partially through modulating SMH1stability and activity.

INTRODUCTION

Soil salinity is a significant and growing abiotic stress worldwide, reducing crop growth and productivity. One of the consequences of the buildup of sodium in the soil is the accumulation of high concentrations of sodium ions (Na^+) in the cell (Hasegawa et al., 2000). Cellular Na^+ affects almost all aspects of cell function likely due to the replacement of essential potassium ions (K^+) by Na^+. Therefore, maintenance of Na^+/K^+ homeostasis is critical for plant growth and development (Munns and Tester, 2008). Previous studies have demonstrated that the salt stress–induced Salt Overly Sensitive (SOS) pathway is essential for plant Na^+/K^+ homeostasis in *Arabidopsis thaliana* (Zhu, 2003). SOS3 and SOS3-like Calcium Binding Protein8 (SCaBP8), two calcium sensors, decode a calcium signal induced by salt stress and physically interact with and activate SOS2, a protein kinase. Subsequently, the SOS3/SCaBP8-SOS2 complex localizes to the plasma membrane (PM) and activates SOS1, a PM Na^+/H^+ antiporter, to transport Na^+ out of cell (Shi et al., 2000; Shi et al., 2002; Qiu et al., 2002). The translocation of Na^+ into vacuoles by vacuolar-localized Na^+/H^+ antiporters, such as At-NHX, provides another mechanism to prevent the toxic accumulation of Na^+ in the cytoplasm (Apse et al., 1999; Yokoi et al., 2002; Apse et al., 2003; An et al., 2007; Barragán et al., 2012). Voltage-dependent cation channels (HKT and KUP), proton pumps (the H^+-ATPase and the H^+-pyrophosphatase) and a Ca^{2+}/H^+ antiporter (VCX1) also play roles in Na^+ compartmentation (Assmann and Haubrick, 1996; Serrano et al., 1999; Gaxiola et al., 2001; Senn et al., 2001; Berthomieu et al., 2003; Rus et al., 2004; Davenport et al., 2007; Fuglsang et al., 2007; Yang et al., 2010).

In addition to disruption of ion homeostasis, another effect of elevated concentrations of Na^+ in the cytoplasm is the accumulation of disordered/unfolded proteins. These altered proteins induce endoplasmic reticulum stress that triggers their degradation by the 26S proteasome (Liu et al., 2011). Recently, it has been shown that endoplasmic reticulum–associated degradation of proteins is critical for plant salt tolerance (Liu et al., 2011; Cui et al., 2012) and that protein modification by ubiquitination is

[1] These authors contributed equally to this work.
[2] Address correspondence to guoyan@cau.edu.cn.
The author responsible for distribution of materials integral to the findings presented in this article in accordance with the policy described in the Instructions for Authors (www.plantcell.org) is: Yan Guo (guoyan@cau.edu.cn).
[C] Some figures in this article are displayed in color online but in black and white in the print edition.
[W] Online version contains Web-only data.
www.plantcell.org/cgi/doi/10.1105/tpc.112.106393

essential for disordered/unfolded protein degradation. Ubiquitin (Ub), a small peptide of 76 amino acids, is transferred to specific substrates through a cascade of reactions mediated by E1 (Ub-activating enzyme), E2 (Ub-conjugating enzyme), and E3 (Ub ligase) (Hochstrasser, 1996). Substrates to which mono- or polyubiquitin have been attached participate in different cellular processes: While monoubiquitination modulates protein subcellular location and enzyme activity, polyubiquitinated proteins are subject to 26S/Ub proteasome–mediated degradation (Haglund and Dikic, 2005; Welchman et al., 2005).

Ubiquitination is a reversible process in which deubiquitination enzymes (DUBs) cleave the conjugated Ub from its target protein. DUBs perform other activities, including generation of mature Ub from Ub precursors or recycling of Ub by disassembling freed poly-Ub chains (Wilkinson, 2000; Wing, 2003; Amerik and Hochstrasser, 2004). One class of Cys protease DUBs in *Arabidopsis*, the ubiquitin-specific proteases (UBPs), contains 27 genes grouped into 14 subfamilies all possessing a signature Cys and His box. Although little is known about the specific substrates of each member, a few UBPs have been reported to be involved in the regulation of plant growth, development, and gene expression. For example, UBP14 is involved in root responses during phosphate deficiency (Li et al., 2010), while UBP26 is required for seed development and the repression of PHERES1 (Luo et al., 2008). UBP26 also plays a role in chromatin remodeling affecting small interfering RNA–mediated heterochromatin formation as well as FIS Polycomb repression (Sridhar et al., 2007). UBP15 is required for cell proliferation, flowering, and apical dominance (Liu et al., 2008), and UBP3 and UBP4 are essential for pollen development and transmission (Doelling et al., 2007). With the exception of UBP26, which can deubiquitinate H2B, targets of other UBPs in *Arabidopsis* are not known.

Increased reactive oxygen species (ROS) formation is observed in response to both the osmotic and ionic stresses associated with soil salinity (De Gara et al., 2010). It has been reported that a mutation in SERINE HYDROXYMETHYLTRANSFERASE1 (*shm1-2*, a weak allele) leads to overaccumulation of ROS and that the mutant is more sensitive to salt stress and pathogens than is the wild type (Moreno et al., 2005). The *Arabidopsis* genome encodes seven *SHM* genes, and few of these gene products have been shown to function in mitochondria (McClung et al., 2000; Bauwe and Kolukisaoglu, 2003; Jamai et al., 2009; Engel et al., 2011). SHM1 is the major SERINE HYDROXYMETHYLTRANSFERASE (SHMT) isozyme in *Arabidopsis* leaves (Somerville and Ogren, 1981; McClung et al., 2000); the *shm1-1* mutant was the first photorespiratory mutant identified in *Arabidopsis*. In *shm1-1* plants, leaf mitochondrial SHMT activity was undetectable and photorespiratory Gly metabolism to Ser was significantly reduced (Somerville and Ogren, 1981). These results suggest that maintaining both photosynthetic and photorespiratory activities is important in the response of the plant to salt (Hoshida et al., 2000; Allakhverdiev et al., 2001; Vidal et al., 2007; Timm et al., 2008) because altering either activity results in plant growth inhibition, likely due to overaccumulation of ROS in the chloroplast and mitochondria (Torres, 2010).

In this study, we show that *Arabidopsis* UBP16 is required for plant salt tolerance through its regulation of PM Na^+/H^+ antiport activity and SHM1 activity. UBP16 modulates deubiquitination of SHM1 in planta, which regulates its stability and activity. These results suggest that deubiquitination of Ub-conjugated components of the photorespiratory pathway is critical for maintenance of Na^+/K^+ homeostasis and repression of cell death during salt stress.

RESULTS

The *ubp16* Mutant Is Hypersensitive to Salt

We previously reported a systematic analysis of the UBP gene family in *Arabidopsis* (Liu et al., 2008). To further determine the specific function of each At-UBP member, T-DNA mutants were analyzed for their growth in response to salt. The *ubp16* mutant exhibited reduced salt tolerance. The T-DNA insertion in this mutant (*ubp16*/SALK_023552) is located in the sixth exon of *UBP16* and was confirmed by PCR using a *UBP16*-specific primer and the T-DNA left border primer. The absence of full-length *UBP16* transcript in the *ubp16* mutant was confirmed by RT-PCR analysis (Figure 1A).

When 5-d-old mutant and wild-type (Columbia-0 [Col-0]) seedlings were transferred to Murashige and Skoog (MS) medium with 100 mM NaCl, primary root growth of *ubp16* was indistinguishable from Col-0; however, shoot tissues showed a significant reduction in growth (Figure 1B). At this concentration of salt, fresh weight in the mutant decreased 30% compared with growth in Col-0 (Figure 1C). When seedlings were grown on 120 mM NaCl, growth inhibition was more pronounced and root growth was also inhibited (Figures 1B and 1C).

To complement the *ubp16* salt-sensitive phenotype, a 7664-bp genomic DNA fragment (corresponding to the sequence from 1930 bp upstream of the *UBP16* translation start codon to 698 bp downstream of the stop codon) was cloned into the *pCAMBIA1200* vector. The resulting construct was transformed into the *ubp16* mutant. T3 transgenic lines treated with salt demonstrated that the transgene rescued the mutant phenotype to wild-type salt tolerance (Figures 1D and 1E). These results demonstrate that the NaCl sensitivity of *ubp16* is due to loss of UBP16 function. The transcription levels of *UBP16* in the transgenic lines were similar to or lower than levels in Col-0 (see Supplemental Figure 1A online). The salt-sensitive phenotype of *ubp16* was also observed in soil when plants were treated with 150 mM NaCl for 2 weeks. Under these conditions, shoot growth and chlorophyll content were significantly reduced (see Supplemental Figures 1B and 1C online). Among members of the At-UBP family, UBP16 shares the highest sequence similarity with UBP17 (see Supplemental Figure 2A and Supplemental Data Set 1 online). However, the *ubp16 ubp17* double mutant was not more sensitive to salt than the *ubp16* single mutant (see Supplemental Figures 2B and 2C online), suggesting that UBP16 and UBP17 do not function redundantly in response to salt.

To determine whether *ubp16* is specifically sensitive to Na^+, Col-0 and *ubp16* seedlings were treated with 100 mM KCl, 100 mM $NaNO_3$, 10 mM LiCl, or 3 mM CsCl. The *ubp16* mutant was sensitive to 100 mM $NaNO_3$ and 10 mM LiCl but did not show significant reductions in growth on medium containing 100 mM KCl or 3 mM CsCl, suggesting that *ubp16* is specifically sensitive to Na^+ but not K^+ or Cl^- (see Supplemental Figure 3 online).

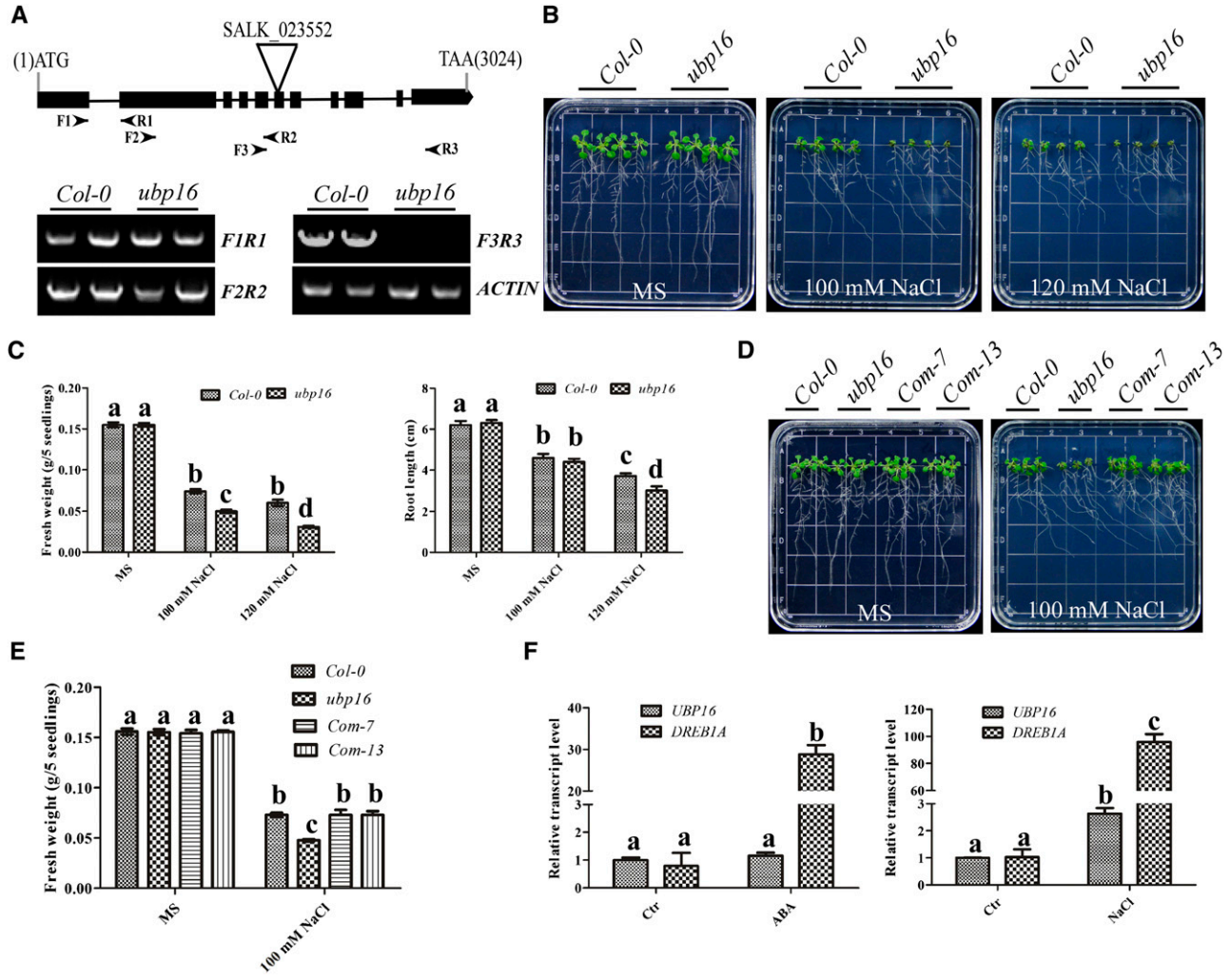

Figure 1. The *Arabidopsis ubp16* Mutant Is Hypersensitive to Salt.

(A) Schematic structure of *UBP16* and RT-PCR analysis. Filled black boxes, exons; lines between boxes, introns; triangle, T-DNA insertion site; arrowheads, primers used to identify the T-DNA insertion and to monitor the level of *UBP16* transcription. RT-PCR analysis was used to monitor the expression of *UBP16* in the wild-type and *ubp16* mutant. *ACTIN* was used as a loading control. Similar results were obtained in three independent replicate experiments.

(B) Analysis of salt sensitivity in wild-type (Col-0) and *ubp16* mutant seedlings. Five-day-old Col-0 and *ubp16* mutant seedlings grown on MS medium were transferred to MS medium without or with 100 or 120 mM NaCl. Photographs were taken 10 d after transfer.

(C) Analysis of seedling fresh weight and root length for seedlings in **(B)**. Error bars represent SD ($n > 10$). Statistical significance was determined by a Student's *t* test; significant differences ($P \leq 0.05$) are indicated by different lowercase letters.

(D) Complementation of the *ubp16* mutant with the wild-type *UBP16* genomic sequence. Five-day-old seedlings from Col-0, the *ubp16* mutant, and two independent complemented lines (*Com-7* and *Com-13*) grown on MS medium were transferred to MS medium without or with 100 mM NaCl. Photographs were taken 10 d after transfer.

(E) Analysis of fresh weight for seedlings in **(D)**. Error bars represent SD ($n > 10$). Statistical significance was determined by a Student's *t* test; significant differences ($P \leq 0.05$) are indicated by different lowercase letters.

(F) Expression of *UBP16* in response to ABA and NaCl. Real-time PCR analysis with *ACTIN* as the internal control. *DREB1A*, a stress-responsive gene, was used as a positive control. Error bars represent SD ($n > 6$). Statistical significance was determined by a Student's *t* test; significant differences ($P \leq 0.05$) are indicated by different lowercase letters.

[See online article for color version of this figure.]

To determine if expression of *UBP16* is regulated by exposure to salt, total RNA was extracted from Col-0 plants treated for 6 h with 100 mM NaCl or 20 μM ABA. The expression of *UBP16* was induced by NaCl but not ABA treatment as determined by real-time RT-PCR analysis. As a control, the *DREB1A* transcription factor was included and its expression was induced by both NaCl and ABA treatments (Figure 1F). *UBP16* was expressed in flowers, siliques, rosette leaves, cauline leaves, stems, and roots (see Supplemental Figure 4A online). UBP16 promoter activity was analyzed using 1930 bp of the *UBP16* promoter fused to the β-*GLUCURONIDASE* (*GUS*) reporter gene. The resulting constructs were transformed into the Col-0 background. For each construct, 12 independent T2 transgenic lines were analyzed for GUS staining. Consistent with the real-time RT-PCR results, GUS expression driven by the *UBP16* promoter was strong in flowers, siliques, and leaves and weak in roots (see Supplemental Figure 4B online).

UBP16 Possesses Deubiquitination Activity

UBP subfamily proteins contain a conserved Cys box that is essential for their DUB activity (Figure 2A) (Liu et al., 2008). To determine if UBP16 possesses DUB enzyme activity, UBP16 was translationally fused to a maltose binding protein tag. A mutated form of UBP16 in which the conserved catalytic Cys at residue 551 (Cys-551) was changed to Ser was created as a control. The two constructs were coexpressed with polyhistidine-tagged UBIQUITIN EXTENSION PROTEIN1 (UBQ1; a model substrate) in *Escherichia coli*. Immunoblot analysis with an anti-Ub antibody showed that UBP16 cleaved UBQ1 but UBP16^{Cys551Ser} did not, suggesting that UBP16 is a DUB and that Cys-551 is essential for its DUB activity (Figure 2B). To further determine if the DUB activity of UBP16 is required for its function in salt tolerance, a Cys^{551Ser} mutation was generated in UBP16 based on the UBP16 complementation plasmid, and the resulting construct was transformed into the *ubp16* mutant. When T3 transgenic lines were treated with salt, lines expressing the mutated *UBP16* gene did not rescue the salt-sensitive phenotype of the *ubp16* mutant (Figures 2C and 2D), even though the mutated gene was expressed at a similar level to *UBP16* in Col-0 (see Supplemental Figure 5 online). When used as a control, wild-type UBP16 was found to rescue the mutant phenotype (Figures 2C and 2D).

UBP16 Positively Regulates PM Na^+/H^+ Antiport Activity

To examine if Na^+/K^+ homeostasis is impaired in the *ubp16* mutant during salt stress, 3-week-old soil-grown Col-0 and *ubp16*

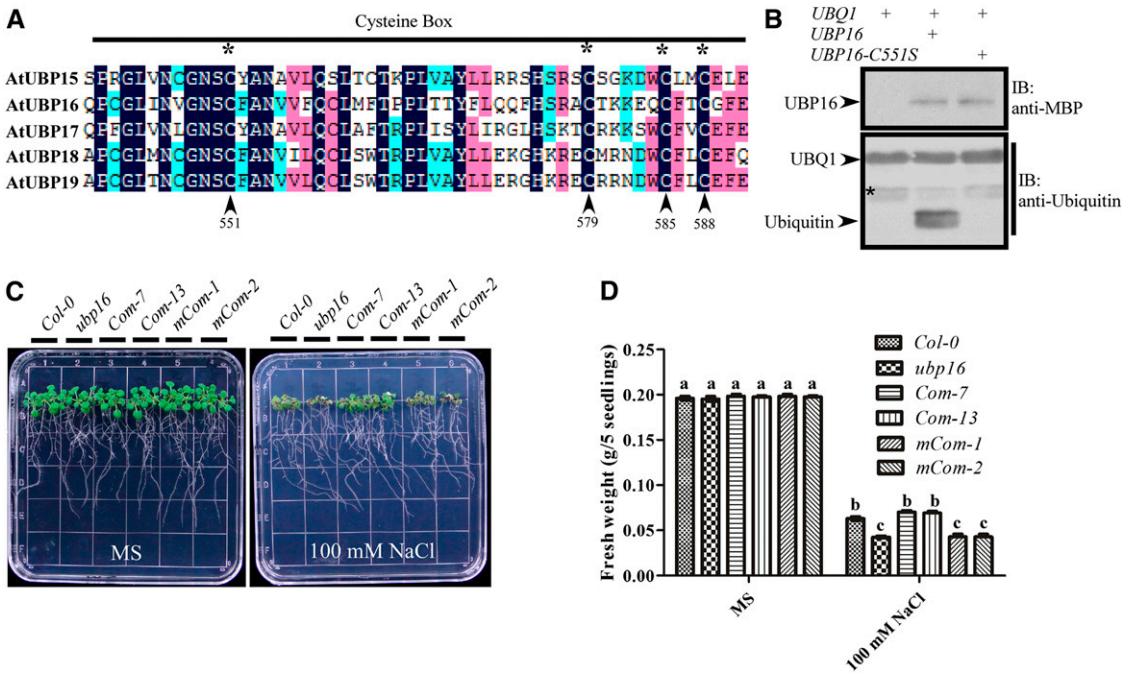

Figure 2. UBP16 Is a UBP Enzyme in *Arabidopsis*.

(A) Schematic representation of the Cys box of five related At-UBPs. Asterisks and arrowheads indicate the conserved Cys residues in the Cys box.
(B) Analysis of deubiquitination activity in vitro. UBQ1 was used as the substrate and was expressed alone or coexpressed with wild-type UBP16 or UBP16^{Cys551Ser} in *E. coli* (DE3) cells. Experimental details are provided in Methods. Anti-MBP antibody and anti-Ub antibodies were used to detect UBP16 and the Ub signal, respectively. The asterisk indicates a nonspecific band associated with the anti-Ub antibody. IB, immunoblot.
(C) Analysis of salt sensitivity in two independent complemented lines expressing Cys^{551Ser} in the *UBP16* genomic sequence. The two lines complemented with the wild-type *UBP16* gene used in Figure 1D were used as controls. Five-day-old seedlings grown on MS medium were transferred to MS medium without or with 100 mM NaCl. Photographs were taken 10 d after transfer.
(D) Analysis of fresh weight for seedlings in **(C)**. Error bars represent SD ($n > 10$). Statistical significance was determined by a Student's *t* test; significant differences ($P \leq 0.05$) are indicated by different lowercase letters.
[See online article for color version of this figure.]

plants were exposed to 150 mM NaCl for 10 d, and Na^+ and K^+ content was measured. Na^+ content increased in both plants and was significantly higher in *ubp16* than in Col-0 (Figure 3A). By contrast, K^+ content was significantly lower in *ubp16* than in Col-0 under control conditions and decreased in both plants after NaCl treatment (Figure 3A). These results suggest that UBP16 inhibits Na^+ accumulation and enhances K^+ accumulation. To determine if PM Na^+/H^+ antiport activity is altered in the *ubp16* mutant, PM vesicles were isolated from mutant and wild-type seedlings treated with 250 mM NaCl for 3 d. Na^+/H^+ antiport activity was significantly lower in *ubp16* plants than in Col-0 plants at all concentrations of NaCl assayed (Figures 3B and 3C). These data demonstrate that UBP16 is required for the regulation of PM Na^+/H^+ antiport activity.

Because the *ubp16* mutant accumulated less K^+ than Col-0 even in control conditions (Figure 3A), we determined if growth

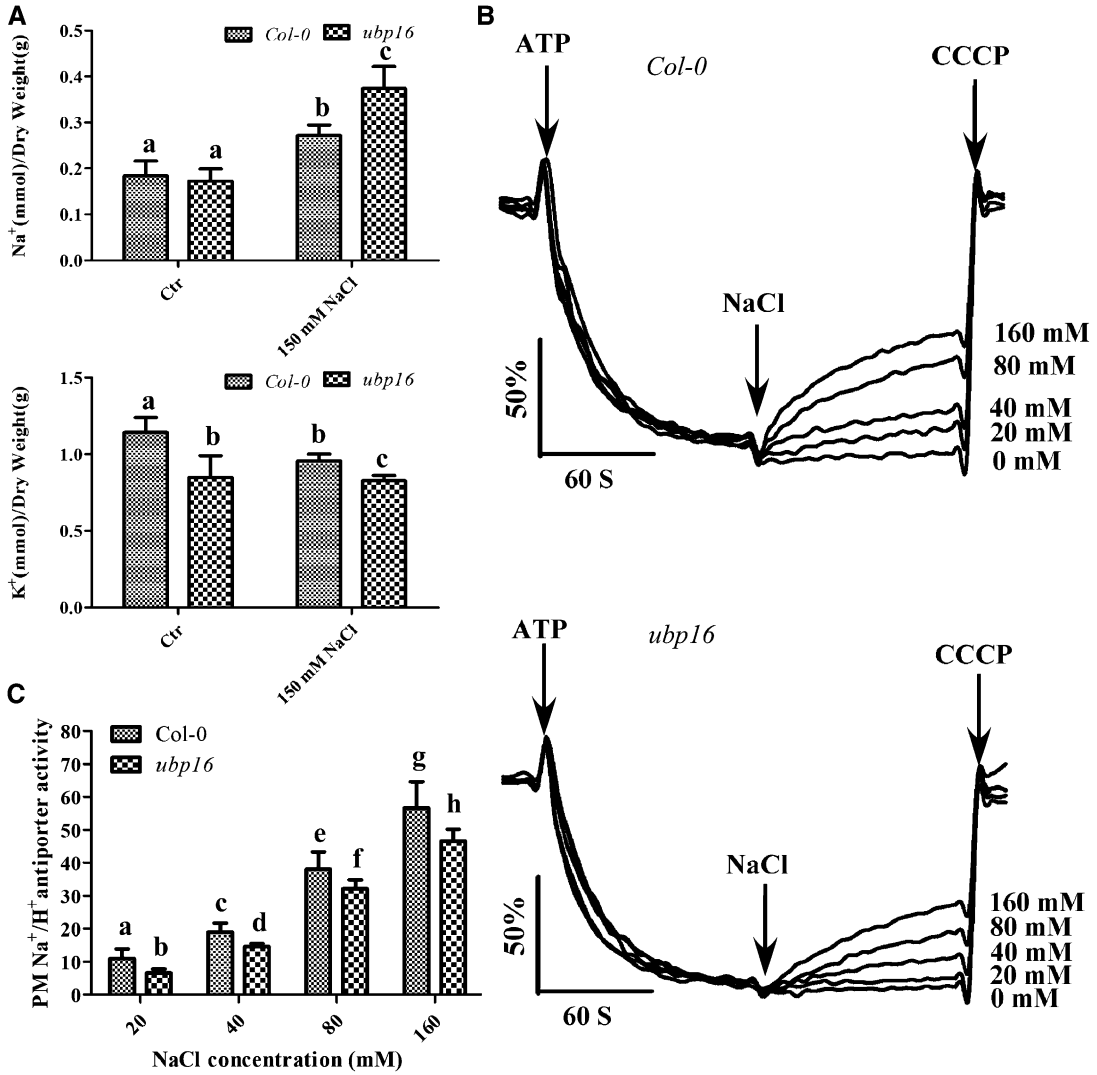

Figure 3. UBP16 Positively Regulates PM Na^+/H^+ Antiport Activity in *Arabidopsis*.

(A) Na^+ and K^+ accumulation in Col-0 and the *ubp16* mutant was determined with an atomic absorption spectrophotometer (Hitachi Z-5000). Details are provided in Methods. Error bars represent SD ($n > 6$). Statistical significance was determined by a Student's *t* test; significant differences ($P \leq 0.05$) are indicated by different lowercase letters. Ctr, control.

(B) Analysis of PM Na^+/H^+ antiport activity in Col-0 and the *ubp16* mutant. PM vesicles were isolated from 3-week-old soil grown seedlings of Col-0 and the *ubp16* mutant treated with 250 mM NaCl for 3 d. PM ATPase activity was initiated by the addition of 3 mM ATP, and the indicated concentrations of NaCl were added to monitor the Na^+/H^+ transport activity of the antiporter. The pH gradient was collapsed with the addition of 10 mM carbonyl cyanide *m*-chlorophenyl hydrazine (CCCP). Details are provided in Methods.

(C) Comparison of PM Na^+/H^+ antiport activity in Col-0 and the *ubp16* mutant. Error bars represent SD ($n = 5$) of at least three replicate experiments, each from an independent isolation of PMs. Statistical significance was determined by a Student's *t* test; significant differences ($P \leq 0.05$) are indicated by different lowercase letters.

of the *ubp16* mutant is altered under low K^+ conditions. Five-day-old *akt1* (an AKT1 K^+ channel mutant), *cipk23* (a mutant in CALCINEURIN B-LIKE-INTERACTING PROTEIN KINASE23, a regulator of AKT1) and a *CIPK23* overexpression line (all of which have been characterized for their responses in low K^+ conditions; Xu et al., 2006), along with the *ubp16* mutant and Col-0 plants, were transferred to low K^+ medium containing 100 or 140 μM KCl. Consistent with previous reports, *akt1* and *cipk23* were more sensitive and the *CIPK23* overexpression line was more tolerant to these conditions than the wild type. Under these conditions, growth of the *ubp16* mutant was not significantly different than the growth of Col-0 (see Supplemental Figure 6 online).

UBP16 Functions in Parallel with SCaBP8 to Regulate Salt Tolerance

It has been shown that SCaBP8 functions mainly in shoot tissue to protect *Arabidopsis* from salt stress by interacting with SOS2 and activating SOS1 in the PM (Quan et al., 2007; Lin et al., 2009). The *ubp16* mutant was less sensitive to NaCl than *scabp8* but had a similar pattern of growth defect (Figure 4A). To determine if UBP16 interacts genetically with SCaBP8, a *scabp8* T-DNA insertion line (Quan et al., 2007) was crossed with the *ubp16* mutant to generate the *ubp16 scabp8* double mutant. Five-day-old seedlings of the wild type and single and double mutants grown on MS medium were transferred to MS medium without or with 50 or 100 mM NaCl. In the absence of NaCl, none of the mutants showed any significant differences in growth compared with the growth of Col-0. In response to 50 or 100 mM NaCl, shoot growth of the *ubp16 scabp8* double mutant was more severely reduced than in the *ubp16* and *scabp8* single mutants (Figures 4A and 4B). When grown in soil and treated with 150 mM NaCl for 3 or 6 weeks, similar reductions in growth were observed (Figure 4C). Consistent with these observations, UBP16 did not interact with either SCaBP8 or SOS2 in yeast two-hybrid assays (see Supplemental Figure 7A online). These results suggest that SCaBP8 and UBP16 function in parallel to regulate the response of the plant to salt.

UBP16 Interacts with SHM1 and SHM4

To identify possible targets of UBP16, we performed yeast two-hybrid assays using UBP16 as bait. Two positive clones were sequenced and found to be identical to the C termini of At4g37930 and At4g13930, which encode the SHM1 and SHM4 Ser

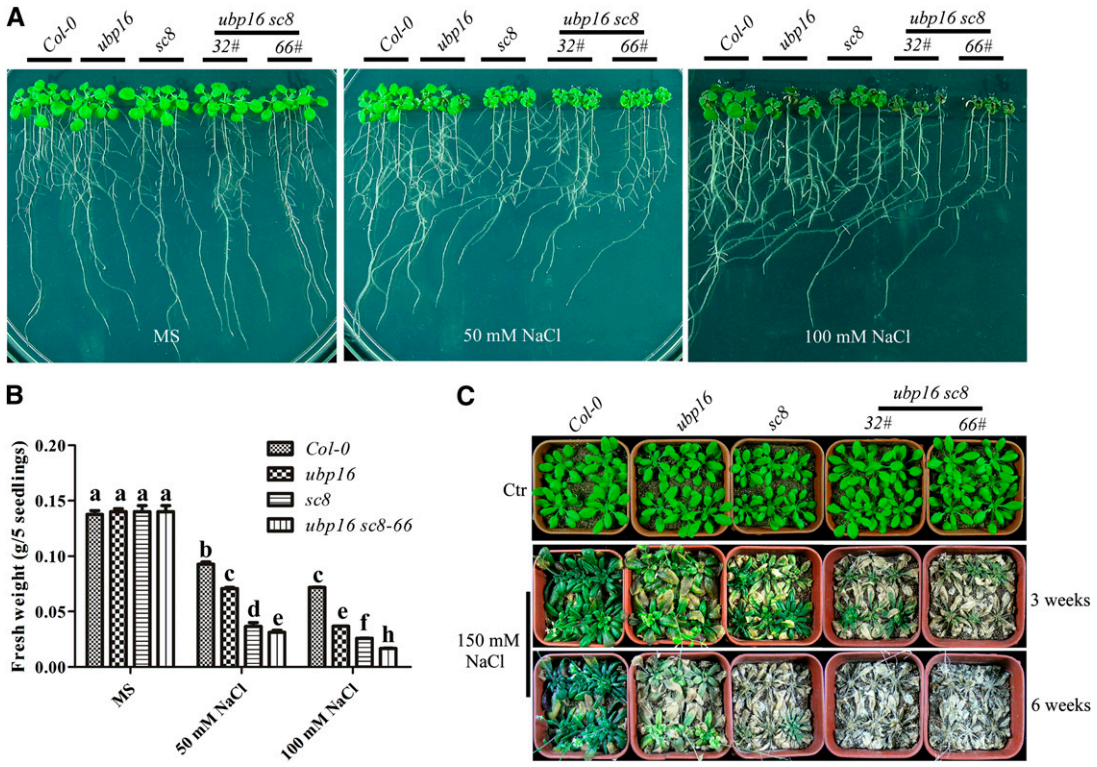

Figure 4. UBP16 and SCaBP8 Function in Parallel in Salt Tolerance in *Arabidopsis*.

(A) Analysis of salt sensitivity in Col-0, *ubp16*, *scabp8* (*sc8*), and the *ubp16 scabp8* (*ubp16 sc8*) double mutant seedlings. Five-day-old seedlings of Col-0, *ubp16*, *sc8*, and two independent lines of the *ubp16 sc8* double mutant grown on MS medium were transferred to MS medium without or with 50 or 100 mM NaCl. Photographs were taken 10 d after transfer.

(B) Analysis of fresh weight for seedlings in **(A)**. Line 66 was chosen as a representative line for the *ubp16 sc8* double mutant. Error bars represent SD ($n > 10$). Statistical significance was determined by a Student's *t* test; significant differences ($P \leq 0.05$) are indicated by different lowercase letters.

(C) Analysis of salt sensitivity in Col-0, *ubp16*, *sc8*, and the *ubp16 sc8* double mutant plants in soil. After 3 weeks of growth in soil, the plants were treated with 150 mM NaCl for 3 or 6 weeks and photographed. Ctr, control photographed before salt treatment.

hydroxymethyltransferases, respectively (see Supplemental Figure 7A online). To narrow down the SHM-interacting domain in UBP16, the UBP16 protein was divided into two parts, UBP16-N (amino acids 1 to 500 including a zinc finger domain) and UBP16-C (amino acids 501 to 1008 including a UB C-terminal hydrolase 2 domain). The structures of the peptides are shown in Figure 5A and Supplemental Figure 7B online. These fragments of *UBP16* were cloned into the *pGADT7* vector, and the full-length *SHM1* and *SHM4* coding sequences were cloned into the *pGBKT7* vector. Combinations of *UBP16* and *SHM1* or *SHM4* were cotransformed into yeast strain AH109. Both SHM1 and SHM4 interacted with the C terminus but not N terminus of UBP16 (Figure 5B; see Supplemental Figure 7C online).

To determine if this interaction takes place in vivo, SHM1- and SHM4-specific antibodies were generated by immunizing mice with *E. coli*–expressed SHM1 and SHM4. To evaluate the specificity of the antibodies, total protein was extracted from Col-0, *shm1-1* (Moreno et al., 2005), and *shm4-1* (SALK_113479, a knockdown mutant; see Supplemental Figure 8A online) and analyzed using immunoblot assays. Strong cross-reaction from both antibodies was detected in Col-0; no cross-reaction was observed in the *shm1-1* mutant with the SHM1 antibody, and weak cross-reaction was detected in *shm4-1* with the SHM4 antibody (Figure 5C). We then fused three Flag tags in a tandem repeat to the UBP16-N or UBP16-C peptides. The resulting *3×Flag-UBP16-N* or *3×Flag-UBP16-C* plasmids were transformed into *Arabidopsis* leaf protoplasts. The 3×Flag-UBP16-N or 3×Flag-UBP16-C peptides were immunoprecipitated with anti-FLAG–conjugated agarose, and coimmunoprecipitating proteins were probed with anti-SHM1 or -SHM4 antibodies. The 3×Flag-UBP16-C protein but not the 3×Flag-UBP16-N protein pulled down both SHM1 and SHM4 (Figure 5D), suggesting that UBP16 interacts with SHM1 and SHM4. Together with the results from the yeast two-hybrid assays, our data indicate that UBP16 and SHM1/SHM4 interact in vivo.

SHM1 Is Localized in Both the Cytosol and Mitochondria

UBP16 is mainly expressed in shoot tissue (see Supplemental Figures 4A and 4B online), and a mutation in *UBP16* resulted in reduced shoot growth in response to salt (Figures 1B to 1D). It has been reported that *SHM1* is also mainly expressed in shoots

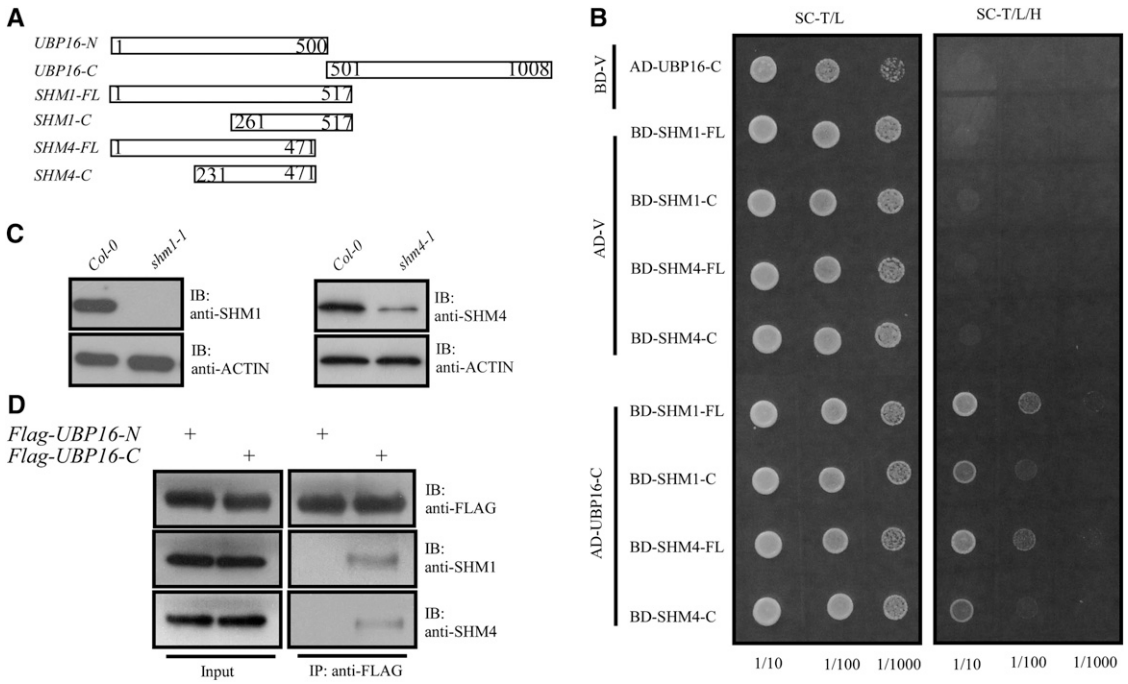

Figure 5. UBP16 Interacts with SHM1 and SHM4.

(A) Schematic diagram of UBP16 (UBP16-FL), the UBP16 C terminus (UBP16-C), the SHM1 N terminus (SHM1-N), the SHM1 C terminus (SHM1-C), the SHM4 N terminus (SHM4-N), and the SHM4 C terminus (SHM4-C).

(B) Analysis of the UBP16 interaction with SHM1 and SHM4 in yeast. Yeast strains expressing the indicated constructs were grown on synthetic complete (SC) medium without Trp and Leu (SC-T/L; left panel) and on SC medium without Trp, Leu, and His (SC-T/L/H; right panel). Pictures were taken after 4 to 5 d of growth on the indicated medium. Panels show yeast serial decimal dilutions.

(C) Analysis of SHM1 and SHM4 antibody specificity. Antibody specificity was tested using immunoblot (IB) assays with total protein extracts from the indicated plants.

(D) Analysis of the interaction between UBP16 and SHM1 or SHM4 in vivo. The *Pro35S:3×Flag-UBP16-N* or *Pro35S:3×Flag-UBP16-C* plasmids were transformed into protoplasts isolated from Col-0. Transiently expressed proteins were immunoprecipitated from total protein extracts (5%; Input) with anti-FLAG agarose and analyzed by immunoblots with anti-FLAG antibody to detect UBP16-N or UBP16-C and anti-SHM1 or anti-SHM4 antibodies to detect the presence of SHM1 or SHM4.

and that the *shm1* mutant is sensitive to salt stress (McClung et al., 2000; Moreno et al., 2005; Voll et al., 2006), while *SHM4* is strongly expressed in the root (McClung et al., 2000). Based on the overlapping expression patterns and mutant phenotypes of UBP16 and SHM1, we focused our studies on the functional interaction between these two proteins. We generated a SHM1 C-terminal green fluorescent protein fusion construct (SHM1-GFP) and both full-length UBP16 N- and C-terminal GFP fusion constructs (GFP-UBP16 and UBP16-GFP) under the control of the cauliflower mosaic virus 35S promoter. The resulting constructs were transformed into *Arabidopsis* Col-0. In T3 transgenic plants, the SHM1-GFP signal partially overlapped with the Mito Tracker Red mitochondrial marker (Figure 6A), which is consistent with a previous report (Jamai et al., 2009). More than 100 independent transgenic lines expressing *GFP-UBP16* or *UBP16-GFP* were tested for UBP16 subcellular localization; however, GFP signal was not detectable in any lines. We also expressed these two plasmids transiently in *Arabidopsis* protoplasts and onion (*Allium cepa*) epidermal cells, but no GFP signal was observed. This lack of expression may be due to the fact that the UBP16 protein is likely too large for the transgene to be expressed in the plant or is degraded by a 26S-independent pathway, as MG132 (a specific 26S proteasome inhibitor) treatment did not lead to recovery of the UBP16 GFP signal.

To further confirm that SHM1 is located in the cytoplasm, cytosolic and mitochondrial fractions were isolated from Col-0 plants and subjected to immunoblot analysis with anti-SHM1 or anti-SHM4 antibodies. Both SHM1 and SHM4 were detected mainly in the cytosol but were found at a lower level in the mitochondrial fraction (Figure 6B). Using the same protein samples, ACTIN and Cytochrome C were found in the cytosolic and mitochondrial fractions, respectively.

UBP16 Modulates SHM1 Stability and Affects Its Subcellular Localization

UBP16 is a Ub-specific protease and interacts with SHM1 in the cytoplasm. To understand the nature of this interaction, we determined if SHM1 levels change in the *ubp16* mutant. Protein was extracted from 10-d-old seedlings of Col-0, *ubp16*, *shm1-1*, and *shm4-1* and analyzed using immunoblot assays. The level of SHM1 protein was significantly reduced in the *ubp16* mutant (Figure 7A), while SHM4 protein levels were similar in Col-0 and *ubp16* (Figure 7B). In addition, SHM1 but not SHM4 protein levels were further reduced in the mutant and the wild type after 9 h of NaCl treatment (Figure 7C). Based on these results, we used a cell-free system (Wang et al., 2009) to determine if the reduction of SMH1 in response to salt involves a 26S proteasome–dependent degradation process and whether UBP16 is required for this process. Protein was extracted from Col-0 and *ubp16* seedlings expressing either the *Pro35S:Flag-HA-SHM1* or *Pro35S:Flag-HA-SHM4* transgenes that had been left untreated or were treated with 40 μM MG132, incubated at 22°C for 15, 30, or 60 min, and then analyzed using immunoblot assays with anti-FLAG antibody. SHM1 degraded rapidly in the samples without MG132 treatment; this degradation was significantly reduced with MG132 treatment (Figure 7D). The degradation of SHM1 was even more dramatic in the *ubp16* mutant

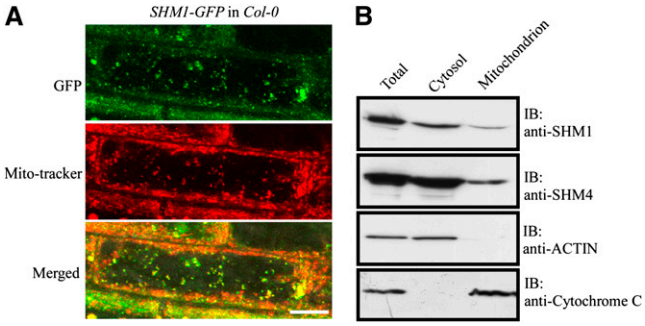

Figure 6. SHM1 Is Localized in Both the Cytosol and Mitochondria in *Arabidopsis*.

(A) Subcellular localization of SHM1-GFP in roots of *Arabidopsis*. Mito-tracker was used as a marker for mitochondria. Bar = 10 μm.

(B) Isolation of cytosolic and mitochondrial fractions. Ten-day-old seedlings of Col-0 were used for cytosol/mitochondria isolation. ACTIN and Cytochrome C were used as cytosol and mitochondrial markers, respectively. IB, immunoblot.

(Figure 7D). SHM4 did not degrade in this assay, and UBP16 did not affect SHM4 stability (Figure 7D). These results suggest that SHM1 undergoes 26S proteasome–dependent degradation and that UBP16 is likely involved in this process.

To determine if SHM1 is ubiquitinated in *Arabidopsis* and if UBP16 plays a role in this ubiquitination/deubiquitination process, Flag-HA-SHM1 was immunoprecipitated by anti-HA antibody–conjugated agarose from the transgenic plants used in Figure 7D. SHM1 loading was determined with anti-FLAG antibody, and Ub conjugation was detected in the immunoprecipitated products using an anti-Ub antibody. SHM1 was polyubiquitinated in *Arabidopsis* (Figure 7E), and this Ub conjugation was higher in the *ubp16* mutant than in Col-0 (Figure 7E). *Pro35S:Flag-HA-SHM1* or *Pro35S:Flag-HA-SOS2* (as a control; Lin et al., 2009) was transformed into *Nicotiana benthamiana* leaves, and transiently expressed Flag-HA-SHM1 and Flag-HA-SOS2 were immunoprecipitated with anti-HA antibody–conjugated agarose. Immunoblot analysis with anti-FLAG or anti-Ub antibody resulted in a ladder of high molecular weight proteins that were detected for SHM1 by both antibodies but not by the anti-Ub antibody for SOS2 (Figure 7F). These results demonstrate that SHM1 is ubiquitinated in planta and that SHM1 deubiquitination involves UBP16.

Our studies have shown that SHM1 is found in both the cytoplasm and mitochondria (Figure 6B). Because ubiquitination is often involved in regulation of protein subcellular localization, we determined if ubiquitination of SHM1 affects its localization. For these assays, mitochondrial fractions were isolated from Col-0 and *ubp16* seedlings left untreated or treated with 100 mM NaCl for 9 h. Consistent with previous results, SHM1 protein levels were reduced in the *ubp16* mutant, and this reduction became more significant in the mitochondrial fraction in response to NaCl treatment (Figure 7G). To determine whether the reduction of SHM1 in mitochondria is due to degradation or a change in subcellular localization, proteins were separated using Suc gradient centrifugation. Total proteins were extracted from Col-0 and *ubp16* plants in mitochondrial isolation buffer, and then protein samples with

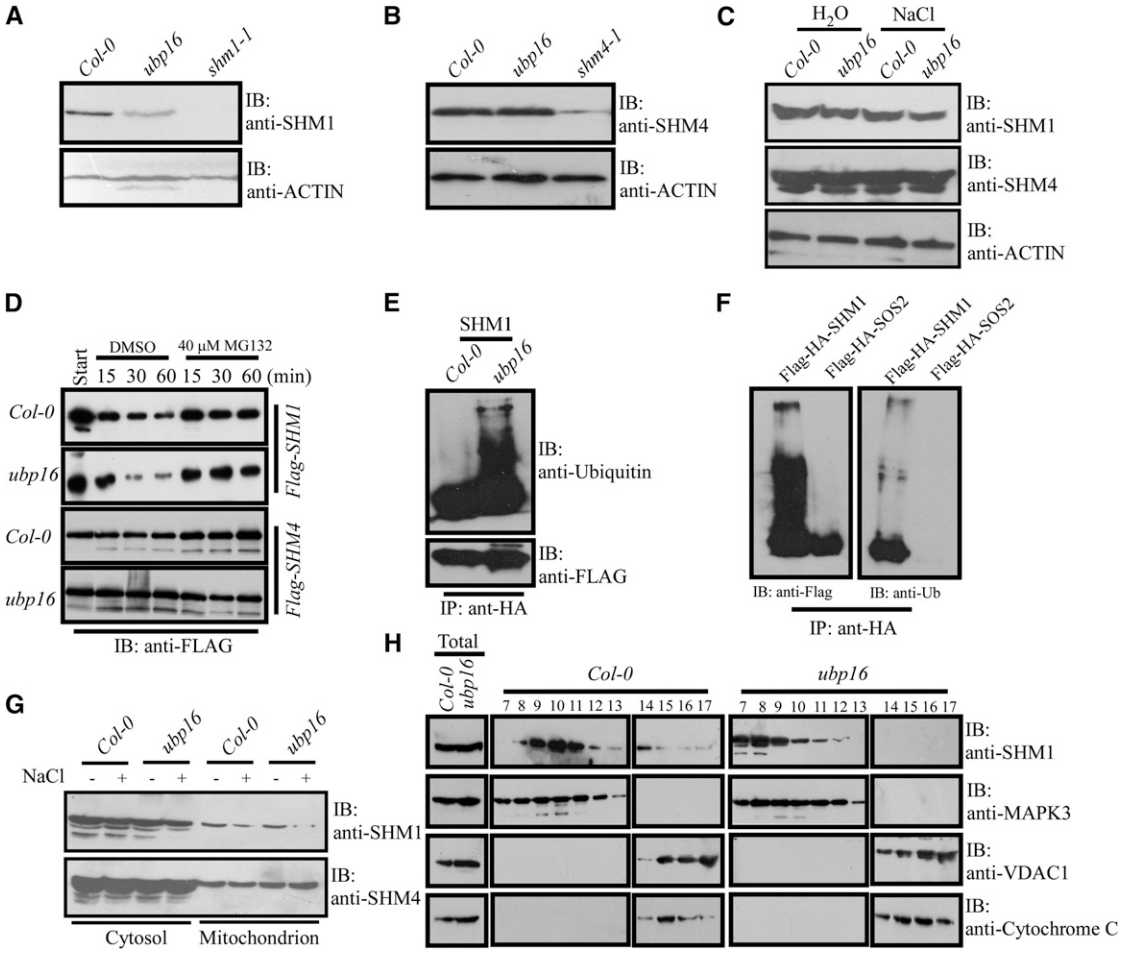

Figure 7. UBP16 Stabilizes SHM1 and Positively Regulates Localization of SHM1 in the Mitochondria in *Arabidopsis*.

(A) Analysis of SHM1 accumulation in the *ubp16* mutant. SHM1 accumulation was determined by immunoblot (IB) analysis with total protein extracts from the indicated plants. ACTIN was used as a loading control.

(B) Analysis of SHM4 accumulation in the *ubp16* mutant. SHM4 accumulation was determined by immunoblot analysis with total protein extracts from the indicated plants. ACTIN was used as a loading control.

(C) Analysis of SHM1 protein stability in response to NaCl treatment. Ten-day-old seedlings were treated with 100 mM NaCl for 9 h, and SHM1 level was determined by immunoblot analysis. SHM4 was used as a control.

(D) Cell-free degradation assay. Ten-day-old seedlings expressing *Pro35S*:*3*×*Flag-HA-SHM1* or *Pro35S*:*3*×*Flag-HA-SHM4* in Col-0 or the *ubp16* mutant were used for cell-free degradation assays using standard protocols (Wang et al., 2009). Anti-FLAG antibody was used to detect SHM1 and SHM4 by immunoblot analysis. MG132, a specific 26S proteasome inhibitor.

(E) Analysis of SHM1 polyubiquitination and the role of UBP16 in this process. Ten-day-old seedlings expressing the *Pro35S*:*Flag-HA-SHM1* transgene in Col-0 or the *ubp16* mutant were used for protein immunoprecipitation with anti-HA antibody-conjugated agarose. Anti-FLAG and anti-Ub antibodies were used to detect Flag-HA–fused proteins and the ubiquitination signal, respectively, via immunoblot assays.

(F) Analysis of the polyubiquitination modification of SHM1 in *N. benthamiana*. *Pro35S*:*Flag-HA-SHM1* or *Pro35S*:*Flag-HA-SOS2* (as a negative control) plasmids were transformed into *N. benthamiana* leaves. Four to five days after infiltration, transiently expressed proteins were immunoprecipitated with anti-HA antibody-conjugated agarose. Immunoblot assays with anti-FLAG and anti-Ub antibodies were used to detect the Flag-HA–fused proteins and Ub-conjugated proteins, respectively.

(G) Isolation of cytosolic and mitochondrial fractions. Seedlings of Col-0 and the *ubp16* mutant were left untreated or treated with 100 mM NaCl for 9 h. SHM4 served as a control. Details are provided in Methods.

(H) Analysis of SHM1 localization in the wild type and the *ubp16* mutant. Suc gradient centrifugation was used to separate cytosolic (7 to 13) and mitochondrial (14 to 17) fractions. MAPK3 was used as cytosol marker, while VDAC1 and Cytochrome C were both used as mitochondrial markers. Details are provided in Methods.

the same amount SHM1 (determined by immunoblot using anti-SHM1 antibodies) were separated by ultracentrifugation in a linear 5 to 50% Suc gradient. Seventeen fractions were collected (numbered from top to bottom) and analyzed using immunoblot analysis with anti-SHM1, -MAPK3, -VDAC (for VOLTAGE-DEPENDENT ANION-SELECTIVE CHANNEL PROTEIN1), and -Cytochrome C antibodies. SHM1 was observed in fractions 8 to 17 in Col-0 and fractions 7 to 12 in the *ubp16* mutant (Figure 7H), and SHM1 protein colocalized with MAPK3, a cytosolic marker. Two mitochondrial markers, VDAC1 and Cytochrome C, were observed in fractions 14 to 17 in both *ubp16* and Col-0 (Figure 7H). In these fractions, SHM1 was detected in Col-0 but was largely absent in *ubp16* (Figure 7H). MAPK3, VDAC1, and Cytochrome C protein levels were slightly higher in *ubp16* than in Col-0 due to the requirement for more total protein for the mutant than for the wild type to equalize the amount of SHM1 protein in both samples. Taken together, these results suggest that UBP16 may be involved in regulating the subcellular localization of SHM1; however, we cannot exclude the possibility that reduced SHM1 stability in the cytosol of the *ubp16* mutant causes reduced accumulation of SHM1 in mitochondria.

UBP16 Modulates Cell Death in Response to Salt Tolerance

It has been reported that mutations in *SHM1* result in sensitivity to salt stress and increased accumulation of hydrogen peroxide (H_2O_2) in leaves in *Arabidopsis* (Moreno et al., 2005). To determine if the *ubp16* mutant has a similar phenotype, we first investigated the H_2O_2 content in Col-0 and *ubp16* by 3,3-diaminobenzidine (DAB) staining. The mutant accumulated higher levels of H_2O_2 than Col-0 after 18 h of treatment with 100 mM NaCl (Figure 8A). Col-0 and *ubp16* mutant seedlings were also treated with 100 mM NaCl for 9 and 18 h, and H_2O_2 content was measured quantitatively with an Amplex Red Kit (Invitrogen). NaCl treatment increased H_2O_2 content in both the mutant and the wild type, with higher levels of H_2O_2 in the mutant before and after NaCl treatment (Figure 8B). When Col-0, *shm1-1*, and *ubp16* seeds were germinated on MS medium without or with 50 or 100 mM NaCl, *shm1-1* seedlings were smaller and chlorotic even on MS medium without salt. Growth of the *shm1-1* mutant was further reduced when seedlings were treated with 50 mM NaCl (Figure 8C), while the *shm4-1* mutant did not display any growth inhibition compared with Col-0 when geminated on MS medium with 50 mM NaCl (see Supplemental Figure 8B online). When treated with 100 mM NaCl, growth of the *ubp16* mutant was reduced more than growth of the *shm1-1* mutant (Figure 8C). These results suggest that UBP16 is involved in salt tolerance partly through modulating SHM1 activity and, at higher NaCl concentrations, through regulating PM Na^+/H^+ antiport activity.

To understand the mechanism by which SHM1 modulates salt tolerance, we monitored trypan blue staining to analyze cell death in Col-0, *ubp16*, *shm1-1*, and *shm4-1*. After treatment with 100 mM NaCl for 24 h, cell death was dramatically induced in *shm1-1*, with slightly less induction in *ubp16* and little induction in Col-0 and *shm4-1* (Figure 8D). We found that salt stress–induced cell death in *ubp16* and *shm1-1* is associated with Cytochrome C release from mitochondria (Figure 8E), a cell death marker (Luo et al., 1998). The Cytochrome C release was induced in *ubp16* and

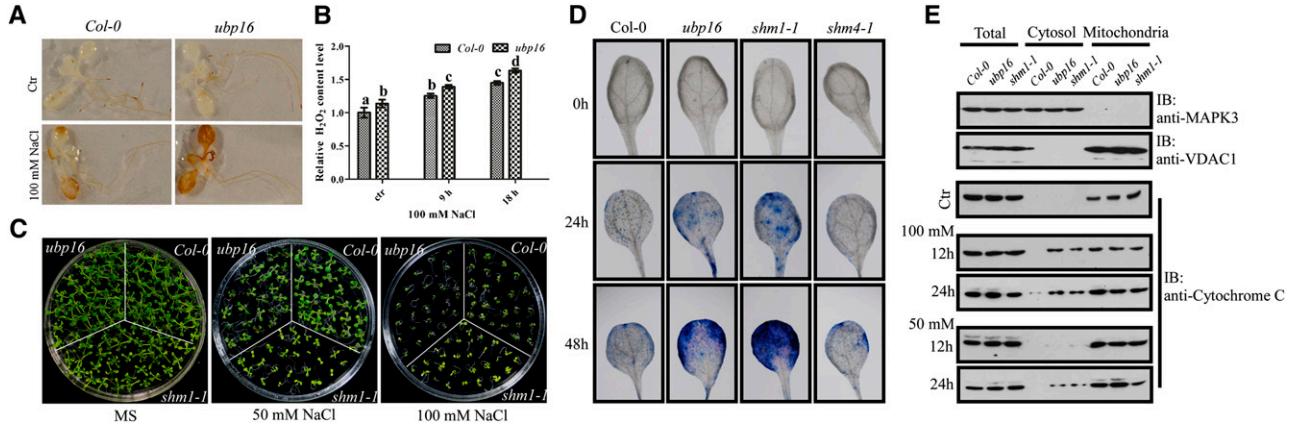

Figure 8. UBP16 and SHM1 Regulate ROS Accumulation and Cell Death in Response to Salt.

(A) DAB staining assay in Col-0 and the *ubp16* mutant. Ten-day-old seedlings were left untreated or treated with 100 mM NaCl for 18 h and stained with DAB to detect endogenous H_2O_2. Ctr, control.

(B) H_2O_2 analysis in Col-0 and the *ubp16* mutant. Ten-day-old seedlings were left untreated or treated with 100 mM NaCl for 9 or 18 h and analyzed for H_2O_2 content with an Amplex Red H_2O_2/peroxidase assay kit. Error bars represent SD (n = 3). Statistical significance was determined by a Student's t test; significant difference ($P \leq 0.05$) is indicated by different lowercase letters.

(C) Analysis of germination in Col-0, *ubp16*, and the *shm1-1* mutant. Seedlings were germinated and grown on MS medium without or with 50 or 100 mM NaCl for 2 weeks and photographed.

(D) Analysis of cell death with trypan blue staining. Ten-day-old seedlings were treated with 100 mM NaCl for 24 or 48 h and stained with trypan blue. Details are provided in Methods.

(E) Detection of Cytochrome C release. Ten-day-old seedlings of Col-0, *ubp16*, and *shm1-1* were treated with 0, 50, or 100 mM NaCl for 12 or 24 h and harvested for subcellular fractionation. Samples were subjected to immunoblot (IB) analysis with anti–Cytochrome C antibody. VDAC1 and MAPK3 were used as mitochondria and cytosol markers, respectively. Details are provided in Methods.

shm1-1 but not in Col-0 by treatment with 100 mM NaCl for 12 h. However, after treatment with 100 mM NaCl for 24 h, a release of Cytochrome C was also detected in Col-0. Treatment with 50 mM NaCl only induced Cytochrome C release from *ubp16* and *shm1-1* after 24 h of treatment. These results indicate that the cell death induced by salt stress in *ubp16* and *shm1-1* is associated with Cytochrome C release from mitochondria and that UBP16 regulates salt tolerance at least partially by modulating cell death through SHM1.

UBP16 Modulates Ser Hydroxymethyltransferase Activity, and SHM1 Regulates PM Na^+/H^+ Antiport Activity

To determine if SHMT activity is affected in the *ubp16* mutant, crude protein extracts were isolated from 10-d-old seedlings of Col-0, *shm1-1*, and *ubp16* and SHMT activity was analyzed following the conversion of radioactive carbon from Ser to methylene tetrahydrofolate (THF) (Geller and Kotb, 1989) (Figure 9A). Consistent with a previous report (Jamai et al., 2009), SHMT activity decreased dramatically in the *shm1-1* mutant compared with Col-0. In the *ubp16* mutant, SHMT activity was reduced to a level lower than in Col-0 but higher than in *shm1-1* (Figure 9B). SHMT activity was reduced in both Col-0 and *ubp16* when seedlings were treated with 100 mM NaCl for 12 h, and the reduction in *ubp16* was more significant than in Col-0 (Figure 9C).

UBP16 regulates both PM Na^+/H^+ antiport and SHMT activities. To determine whether these activity changes in the *ubp16* mutant are due to the defect in SHM1, we tested if SHM1 directly regulates Na^+/H^+ antiport activity. PM vesicles were isolated from seedlings

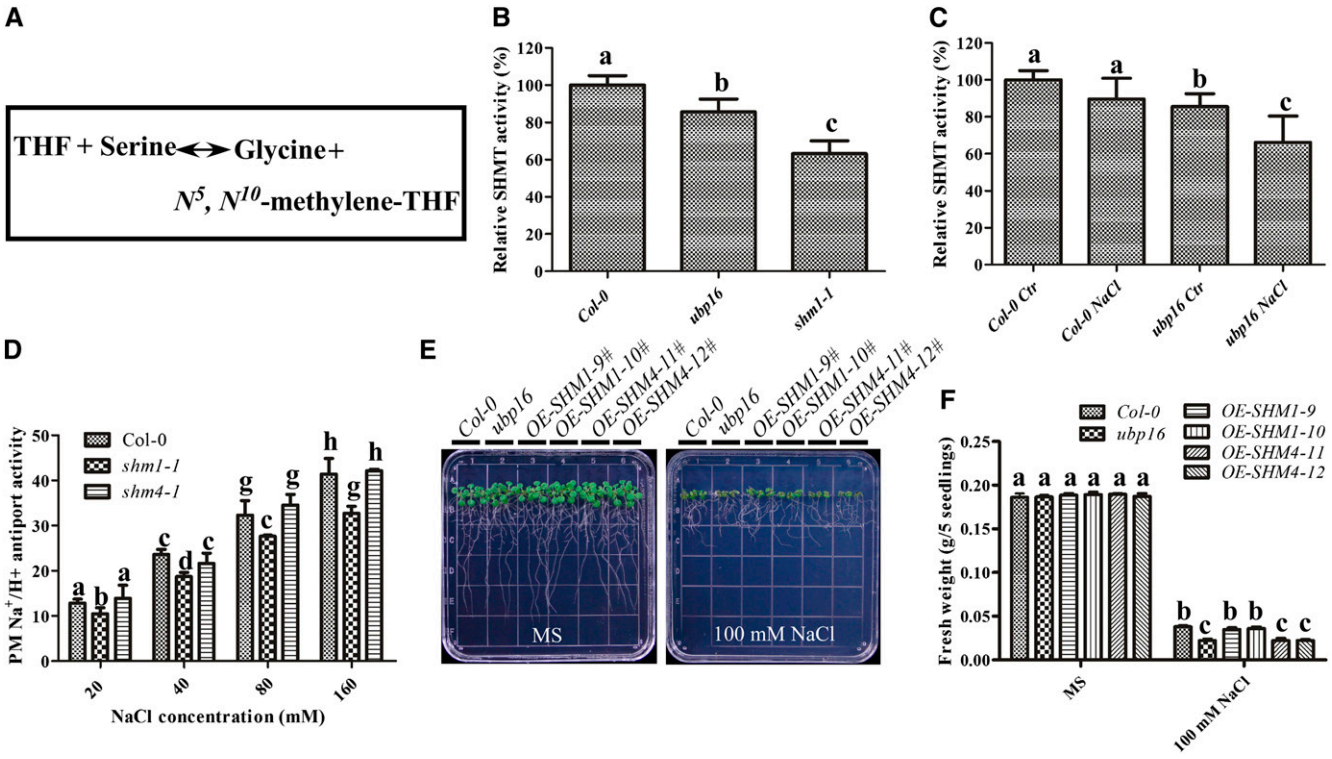

Figure 9. UBP16 Positively Modulates SHMT Activity in *Arabidopsis*.

(A) Schematic representation of the SHMT activity assay. SHMT activity was determined by following the conversion of radioactive carbon from Ser to methylene THF.

(B) SHMT activity assay for Col-0, *ubp16*, and the *shm1-1* mutant. SHMT activity was determined using 400 mg of tissue from 10-d-old seedlings. Error bars represent SD ($n = 3$). Statistical significance was determined by a Student's *t* test; significant difference ($P \leq 0.05$) is indicated by different lowercase letters.

(C) SHMT activity assay for Col-0 and *ubp16* in response to salt. Ten-day-old seedlings were treated with 100 mM NaCl for 12 h, and SHMT activity was determined. Ctr, without NaCl treatment. Error bars represent SD ($n = 3$). Statistical significance was determined by a Student's *t* test; significant difference ($P \leq 0.05$) is indicated by different lowercase letters.

(D) Comparison of PM Na^+/H^+ antiport activity in Col-0, *shm1-1*, and *shm4-1*. Error bars represent SD ($n = 5$) of at least three replicate experiments, each from an independent isolation of PMs. Statistical significance was determined by a Student's *t* test; significant differences ($P \leq 0.05$) are indicated by different lowercase letters.

(E) Analysis of salt sensitivity in Col-0, *ubp16*, and two independent transgenic lines expressing *Pro35S:3×Flag-HA-SHM1* (*9#* and *10#*) or *Pro35S:3×Flag-HA-SHM4* (*11#* and *12#*) in the *ubp16* mutant background. Five-day-old seedlings grown on MS medium were transferred to MS medium without or with 100 mM NaCl. Photographs were taken 8 d after transfer.

(F) Analysis of fresh weight for seedlings in **(E)**. Error bars represent SD ($n > 10$). Statistical significance was determined by a Student's *t* test; significant differences ($P \leq 0.05$) are indicated by different lowercase letters.

[See online article for color version of this figure.]

of Col-0, *shm1-1*, and *shm4-1* treated with 250 mM NaCl for 3 d, and PM Na^+/H^+ antiport activity was analyzed. PM Na^+/H^+ antiport activity in *shm1-1* was significantly lower than in Col-0, while activity in *shm4-1* was similar to that in Col-0 (Figure 9D; see Supplemental Figures 9A to 9C online). These results indicate that SHM1 positively modulates PM Na^+/H^+ antiport activity.

To further confirm that the downregulation of SHMT by the mutation in UBP16 is important for the *ubp16* salt-sensitive phenotype, *Pro35S:Flag-HA-SHM1* and *Pro35S:Flag-HA-SHM4* constructs were generated and transformed into the *ubp16* mutant and Col-0. Overexpression of *SHM1* but not *SHM4* in the *ubp16* mutant partially rescued its salt-sensitive phenotype (Figures 9E and 9F). However, overexpression of *SHM1* and *SHM4* in Col-0 did not confer additional salt tolerance (see Supplemental Figures 8C and 8D online). Protein levels of SHM1 or SHM4 in Col-0 and *ubp16* transgenic plants was similar, as determined by immunoblot analysis with anti-SHM1 or anti-SHM4 antibodies, respectively (see Supplemental Figure 8E online).

DISCUSSION

In this study, we determined that UBP16, a Ub-specific protease, interacted with and stabilized SHM1 and may be required for SHM1 subcellular localization. SHM1 was ubiquitinated and degraded by the 26S proteasome. Consistent with this, *Arabidopsis* plants lacking UBP16 displayed lower SHMT activity, accumulated more salt-induced H_2O_2, and had higher levels of cell death and were more sensitive to salt compared with the wild type. These changes were associated with increased degradation of SHM1 in the cytosol, reduced accumulation in mitochondria, and increased Cytochrome C release from mitochondria. In the *ubp16* mutant, the decrease in SHM1 in both the cytosol and mitochondria is likely at least partly due to the polyubiquitination-triggered protein degradation. However, it needs to be further determined whether UBP16 also affects the monoubiquitination of SHM1 that in turn regulates SHM1 cellular localization and SHMT activity.

The growth inhibition of the *ubp16* mutant in response to salt was mainly observed in shoot tissue and included reduced shoot area and chlorophyll content, changes that are also observed in plants when photorespiration is impaired by salinity (Lakshmi et al., 1996; Misra et al., 1997; Chaves et al., 2009). The salt-sensitive phenotype of the *ubp16* mutant could be due to reduction of SHMT activity and overexpression of *SHM1* in the *ubp16* mutant partially rescued this phenotype. Taken together, our results provide additional evidence that SHMT activity and photorespiration play a critical role in plant salt tolerance and that UBP16 plays a role in this regulation, in part, by modulating SHM1activity. SHM proteins mainly function in mitochondria and mediate ROS generation, which is important in both plant abiotic and biotic stress responses (McClung et al., 2000; Bauwe and Kolukisaoglu, 2003; Moreno et al., 2005; Jamai et al., 2009; Engel et al., 2011). Both *ubp16* and *shm1* mutants accumulated more ROS and a cell death signal (Cytochrome C in the cytoplasm) under salt stress along with more salt-induced cell death than Col-0, suggesting that one explanation for the salt sensitivity of the *ubp16* mutant could be ROS accumulation–induced cell death through the regulation of SHM1.

UBP16 expression was induced by NaCl and the DUB activity of UBP16 was required for its function in salt tolerance. A mutation in *UBP16* leads to a significant reduction in PM Na^+/H^+ antiport activity in response to salt stress. These salt-induced defects are also observed in the *scabp8* mutant, in which SOS1 activity is reduced (Quan et al., 2007). Several lines of evidence suggest that UBP16 regulates Na^+/H^+ antiport activity independently of SCaBP8. First, the *ubp16* mutant accumulated less K^+ than the wild type, while *scabp8* accumulated more K^+ under control conditions (Kim et al., 2007); second, the *ubp16 scabp8* double mutant was more sensitive to salt than either single mutant. Interestingly, PM Na^+/H^+ antiport activity was significantly reduced in *shm1* but not in *shm4*, corresponding to the increase in ROS accumulation in the *shm1* mutant under salt stress. It has been reported that SOS1 interacts with RCD1, a regulator of oxidative stress responses and regulates ROS accumulation under salt stress (Katiyar-Agarwal et al., 2006). Previous data also demonstrated that ROS mediates SOS1 mRNA stability (Chung et al., 2008). These data suggest that ROS plays a critical role in regulating SOS1 activity.

The *Arabidopsis* genome encodes more than 40 Na^+/H^+ antiporters, including eight SOS1 (NHX7) homologs (NHX1-8) (Mäser et al., 2001; Brett et al., 2005). Plants lacking SOS1 have an 80% reduction in PM Na^+/H^+ antiport activity (Qiu et al., 2002), suggesting that SOS1 is the major PM Na^+/H^+ antiporter in *Arabidopsis* and reduction of PM Na^+/H^+ antiport activity in *ubp16* mutant is likely due to a defect of SOS1-related activity. Taken together, our results suggest that UBP16 is induced by salt stress to stabilize SHM1 and reduce ROS accumulation, which in turn represses cell death and activates PM Na^+/H^+ antiport activity (Figure 10).

Measurements of ion content in the *ubp16* mutant suggest that UBP16 inhibits Na^+ accumulation and enhances K^+ accumulation. Under control conditions, K^+ content was significantly

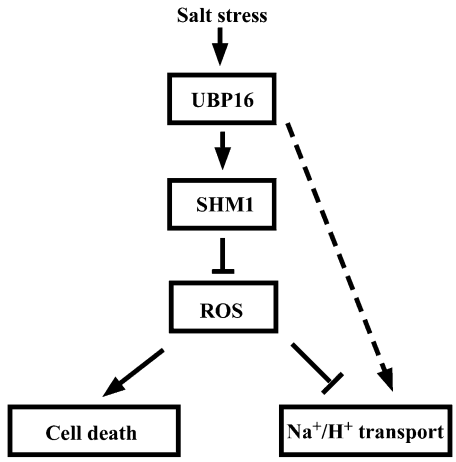

Figure 10. A Working Model for UBP16 and SHM1 Function in Salt Tolerance in *Arabidopsis*.

UBP16 stabilizes SHM1 under salt stress, which represses ROS accumulation and in turn regulates cell viability and PM Na^+/H^+ transport activity. UBP16 may also directly modulate PM Na^+/H^+ antiport/K^+ transport activity independently of SHM1.

lower in the *ubp16* mutant than in Col-0, suggesting that UBP16 may also regulate K^+ channel or K^+ transport activity. K^+ accumulation is reduced in *Arabidopsis* without the AKT1 K^+ transporter (Xu et al., 2006), and these plants are more sensitive to salt (Qi and Spalding, 2004). However, mutants of AKT1 (*akt1*) and its regulators (*cbl1*, *cbl9*, and *cipk23*), defective in high-affinity K^+ transport, are more sensitive to low K^+ (Xu et al., 2006) than the *ubp16* mutant, suggesting that ATK1 may not be a target of UBP16. It is more likely that UBP16 somehow influences low-affinity K^+ transport. However, a possibility that remains to be explored is that, because SOS1 is required for the regulation of PM K^+ transport activity and AKT1 is a possible target of cytosol Na^+ (Qi and Spalding, 2004), UPB16 regulation of PM Na^+/H^+ antiport activity regulates K^+ uptake.

METHODS

Mutants

Arabidopsis thaliana Col-0 was used as the wild type in all experiments. The homozygous *ubp16* mutant was identified from a SALK line (023552) with a T-DNA insertion in the sixth exon of At4g24560. The homozygous *ubp17* mutant was identified from a SALK line (087726). The *shm1-1* mutant was provided by Carmen Castresana (Campus Universidad Autónoma, Madrid, Spain). The *shm4-1* and *scabp8* mutants were identified from SALK T-DNA insertion lines 113479 and 056042, respectively. *ubp16* was crossed with *ubp17* to generate the *ubp16 ubp17* double mutant for salt sensitivity analysis. *ubp16* was crossed with *scabp8* to generate the *ubp16 scabp8* double mutant, and lines 32 and 66 were used in our analyses.

Plant Growth and Analysis of Salt Tolerance

Seeds were sterilized in a solution containing 20% sodium hypochlorite and 0.1% Triton X-100 for 12 min, washed five times with sterilized water, and sown on MS medium with 0.3% (for horizontal growth) or 0.5% (for vertical growth) Phytagel agar (Sigma-Aldrich). Plates were kept at 4°C for 2 d and then seeds were germinated under constant illumination (Philips TLD 30W/54 YZ30RR25) at 23°C.

For salt sensitivity assays on plates, Col-0, the *ubp16* mutant, the *ubp16* complemented lines (*Com-7* and *Com-13*), and the *ubp16 ubp17* and *ubp16 scabp8* double mutants were grown vertically on MS medium with 0.6% agar under continuous light for 5 d at 23°C. Seedlings were transferred to MS medium without or with 100 or 120 mM NaCl. After the indicated times of vertical growth, seedlings were photographed and fresh weight was measured.

For salt sensitivity assays in soil, Col-0, *ubp16*, the *ubp16* complemented lines (*Com-7* and *Com-13*), and the *ubp16 scabp8* double mutant were grown in soil under short-day conditions (8 h light/16 h dark) for 3 weeks. Subsequently, the soil was irrigated with 150 mM NaCl four times every 3 d, and plants were grown for an additional 1 or 4 weeks and photographed and chlorophyll content was analyzed.

Plasmid Construction for Complementation Assays

To complement the *ubp16* mutant, 7664 bp of the *UBP16* genomic sequence was amplified with the GenomicF and GenomicR primers (see Supplemental Table 1 online) and then cloned into the *Kpn*I and *Sal*I sites of the *pCAMBIA1200* vector. The resulting *pCM1200-UBP16* genomic construct was transformed into the *ubp16* mutant. To determine the role of Cys-551 in the deubiquitination activity of UBP16 and in salt tolerance, a Cys^{551Ser} mutation was generated using the *pCM1200-UBP16* genomic plasmid with the mGenomicF and mGenomicR primers (see Supplemental Table 1 online). T3 transgenic lines were confirmed by RT-PCR and lines 7 and 13 (*Com-7* and *Com-13*) from the *pCM1200-UBP16* genomic transformation and lines 1 and 2 (*mCom-1* and *mCom-2*) from the *pCM1200-UBP16*^{Cys551Ser} genomic transformation were used for salt sensitivity assays.

Real-Time and RT-PCR Analysis

Total RNA was extracted with Trizol reagent (Invitrogen) from 10-d-old seedlings grown on MS plates or 1-month-old plants grown in soil in the greenhouse under a 16-h-light/8-h-dark photoperiod. Total RNA was treated with RNase-free DNase I (Takara) to remove genomic DNA. Ten micrograms of RNA was used for reverse transcription with M-MLV reverse transcriptase (Promega) according to the manufacturer's instructions. cDNAs were used for quantitative real-time PCR amplification or RT-PCR analysis with the primers listed in Supplemental Table 2 online. *ACTIN* was used as an internal control.

Analysis of Chlorophyll Content

Leaves were harvested, weighed, and placed into 1.5-mL Eppendorf tubes. Acetone (800 μL of an 80% solution) was added, and the samples were incubated in the dark for 2 h at room temperature. The samples were centrifuged at 15,000*g* for 10 min, and the supernatant was transferred to a new tube. Light absorption at 665 and 649 nm was determined with a microplate reader. The concentration of chlorophyll (total chlorophyll, chlorophyll *a*, and chlorophyll *b*) was calculated according to the following formula: chlorophyll $a = 13.95A665 - 6.88A649$; chlorophyll $b = 24.96A649 - 7.32A665$; and total chlorophyll = chlorophyll *a* + chlorophyll *b*.

Analysis of Subcellular Localization and Promoter Activity

For subcellular localization, the *SHM1* coding region was amplified with the gSHM1F and gSHM1R primers (see Supplemental Table 1 online) and cloned into the *pCM1205-C-GFP* vector using the *Sac*I and *Bam*HI sites to fuse the target protein to the N terminus of GFP. For GUS staining, a 1930-bp genomic DNA fragment from nucleotides 1 to 1930 bp upstream of the translational start site (ATG) of *UBP16* was amplified with the PromoterF and PromoterR primers (see Supplemental Table 1 online) and then cloned into the *Sal*I and *Bam*HI sites of the *pCM1390* vector. The plasmid was transformed into Col-0 and transgenic T3 lines or T2 lines were used for GFP observation or GUS staining, respectively.

Sequence Alignment and Phylogenetic Analysis

Conserved domains of the sequences of the 27 members in the At-UBP protein family were used for phylogenetic analysis. The conserved domains were defined by submitting the protein sequences to both the Pfam (http://pfam.sanger.ac.uk/resources/software/) and the National Center for Biotechnology Information CDART (http://www.ncbi.nlm.nih.gov/Structure/lexington/lexington.cgi?cmd=rps) databases. Alignment of the assembled conserved domains was performed by ClustalW (Thompson et al., 1994). The phylogenetic tree was constructed using MEGA version 3.1 (Kumar et al., 2004) using the neighbor-joining algorithm with 1001 bootstrap replicates.

Analysis of UBP16 Deubiquitination Activity

To detect UBP16-mediated cleavage of Ub linked via α-amino linkages in vivo, MBP-UBP16 or MBP-UBP16^{Cys551Ser} was coexpressed with substrate (His-UBQ1) in *Escherichia coli* DE3 cells. The *E. coli* cells were cultured at 37°C for 4 h to an OD_{600} of 0.8. After subsequent isopropylthio-β-galactoside (1 mM) induction for 3 h, cells were harvested and lysed in SDS loading buffer. The lysates were assayed by immunoblot analysis with anti-Ub and anti-MBP antibodies. An advanced chemiluminescence system (GE Healthcare) was used to detect the signal.

Analysis of Ion Content

Col-0 and the *ubp16* mutant were grown in soil under a 16-h-light/8-h-dark cycle for 3 weeks at 23°C, and the seedlings were treated with 150 mM NaCl for 10 d. Rosette leaves were harvested and dried at 80°C for 2 d. All samples were weighed and treated at 300°C for 1 h and 575°C for 4 h in a muffle furnace. The resulting ground dry matter was dissolved in 0.1 M HCl. The Na^+ and K^+ contents of the samples were determined with an atomic absorption spectrophotometer (Hitachi Z-5000).

PM Isolation and Na^+/H^+ Antiport Activity Assay

Three-week-old plants were used for PM isolation by aqueous two-phase partitioning as described previously (Qiu et al., 2002). PM Na^+/H^+ antiport activity was detected as a Na^+-induced dissipation of the pH gradient as described (Qiu et al., 2002).

Yeast Two-Hybrid Assays

To create the UBP16 bait plasmid, the *UBP16* cDNA was cloned into the *pGBKT7* vector between the *Eco*RI and *Sal*I sites. The N-terminal 500 amino acids of UBP16 (UBP16N) and the C-terminal 508 amino acids of UBP16 (UBP16C) were cloned into the *pGADT7* vector using the *Nco*I and *Sac*I sites. SHM1-FL, containing the 517 amino acids of SHM1; SHM1-C, encoding the C-terminal 257 amino acids of SHM1; SHM4-FL, containing the 471 amino acids of SHM4; and SHM4-C, encoding the C-terminal 241 amino acids were amplified by primers SHM1NF and SHM1CR, SHM1CF and SHM1CR, SHM4NF and SHM4CR, and SHM4CF and SHM4CR, respectively. All fragments were cloned into the *pGBKT7* vector using the *Bam*HI and *Pst*I sites. Yeast transformation and growth assays were performed as described in the Yeast Protocols Handbook (Clontech). All primers used for construction are listed in Supplemental Table 1 online.

Coimmunoprecipitation Assays in Protoplasts

The *UBP16N* and *UBP16C* fragments were amplified with the fhUBP16NF/fhUBP16NR and fhUBP16CF/fhUBP16CR primers (see Supplemental Table 1 online) and inserted into the *pCM1307-N-Flag-HA* vector between the *Sal*I and *Kpn*I sites. CsCl gradient centrifugation-purified plasmids were transformed into protoplasts. Protoplast preparation and transformation were performed using standard protocols (Sheen, 2001). After overnight incubation at 23°C, the protoplasts were lysed, sonicated, and centrifuged. The transiently expressed proteins were extracted using 1 mL immunoprecipitation buffer (10 mM Tris, pH 7.5, 0.5% Nonidet P-40, 2 mM EDTA, 150 mM NaCl, 1 mM PMSF, and 1% protease inhibitor cocktail [Sigma-Aldrich]). The sample was centrifuged at 10,000*g* for 10 min at 4°C to remove cellular debris. Fifty microliters (5%) of the supernatant was collected as input. The rest of the supernatant was transferred to a tube containing 20 μL anti-FLAG agarose (Sigma-Aldrich) and incubated for 2 h at 4°C with gentle rotation. After incubation, the agarose was washed thoroughly approximately four to five times with 1 mL immunoprecipitation buffer per wash. All the immunoprecipitation steps were performed on ice or at 4°C. Proteins were detected by immunoblot analysis with anti-FLAG, anti-SHM1, and SHM4 antibodies.

Antibody Preparation and Analysis

Recombinant SHM1 and SHM4 proteins prepared from *E. coli* were used as antigens for polyclonal antibody production in mouse. The *SHM1* and *SHM4* coding sequences were amplified with the SHM1F/SHM1R and SHM4F/SHM4R primers, respectively, and cloned into the modified *pMAL-p2x* vector between the *Bam*HI and *Xho*I sites. Protein induction and purification was performed according to protocols from NEB. Recombinant proteins were purified with amylose resin, and 2 mg of purified recombinant protein was used for mouse immunization. Serum after immunization was used for antibody tests with samples from plant tissues from Col-0 and the *shm1-1* and *shm4-1* mutants.

Suc Gradient Centrifugation

Ten-day-old seedlings of Col-0 and the *ubp16* mutant were harvested and homogenized in mitochondrial isolation buffer (0.4 M mannitol, 1 mM EGTA, 20 mM β-mercaptoethanol, 50 mM Tricine, and 0.1% BSA, pH 7.8). The homogenate was centrifuged at 4°C at 10,000*g* for 10 min to remove cell debris. The supernatant was overlaid on the top of a 5 to 50% linear Suc gradient and centrifuged at 100,000*g* for 16 h at 4°C. After centrifugation, 250 μL of each fraction was collected and subjected to SDS-PAGE and immunoblot analysis with anti-SHM1 antibody. The VDAC1 and Cytochrome C proteins were used as markers for mitochondria, while MAPK3 and ACTIN were used as cytosolic markers. Anti-VDAC1 antibody was purchased from Agrisera (catalog number AS07212).

Analysis of H_2O_2 Accumulation

H_2O_2 accumulation was measured using two approaches. For DAB staining assays, seedlings grown on MS plates for 10 d were left untreated or treated with 100 mM NaCl for 18 h and then incubated in staining buffer (0.1 mg/mL DAB dissolved in 0.1M HCl, pH 5.0). After 8 h, seedlings were destained (acetic acid:glycerin:ethanol = 1:1:3). For the Amplex Red H_2O_2/peroxidase assay, 10-d-old seedlings were left untreated or treated with 100 mM NaCl for 9 or 18 h and harvested. Detection of H_2O_2 accumulation was performed following the manufacturer's instructions.

Cell-Free Degradation Assay

Ten-day-old *Arabidopsis* Col-0 seedlings were harvested and ground to fine powder in liquid nitrogen. Total proteins were extracted in degradation buffer containing 25 mM Tris-HCl, pH 7.5, 10 mM NaCl, 10 mM $MgCl_2$, 4 mM PMSF, 5 mM DTT, and 10 mM ATP as described (Wang et al., 2009). Cell debris was removed by two 10-min centrifugations at 17,000*g* at 4°C. The supernatant was collected and protein concentration was determined using the Bio-Rad protein assay. MG132 (Calbiochem) was added to the degradation assays as indicated. All mock controls used an equal amount of solvent for each drug. The mixtures were incubated at 22°C, and samples were collected at the indicated times for determination of SHM1 and SHM4 abundance by immunoblot assays.

Cellular Fractionation and Detection of Cytochrome C Release

Ten-day-old *Arabidopsis* seedlings of Col-0, *ubp16*, and *shm1-1* were left untreated or treated with 50 or 100 mM NaCl for 12 or 24 h and ground in homogenization buffer (0.4 M mannitol, 1 mM EDTA, 50 mM Tricine, 20 mM β-mercaptoethanol, and 0.1% BSA, pH 7.8) for 1 min at 4°C. Extracts were centrifuged at 15,000*g* for 5 min at 4°C. Five percent of the supernatant was collected as the total fraction. The supernatant was centrifuged at 16,000*g* for 15 min at 4°C. After this two-step centrifugation, the supernatant was collected as the cytosolic fraction and the pellet was resuspended in homogenization buffer and collected as the mitochondrial fraction. Samples of total, cytosolic, and mitochondrial fractions were subjected to SDS-PAGE and immunoblot analysis with anti–Cytochrome C antibody. VDAC1 was used as a marker for mitochondria and MAPK3 as a marker for the cytosol.

Analysis of Cell Death with Trypan Blue Staining

Trypan blue staining is used for assessing cell death in *Arabidopsis*. Ten-day-old *Arabidopsis* seedlings of Col-0, *ubp16*, *shm1-1*, and *shm4-1* were left untreated or treated with 100 mM NaCl for 24 or 48 h and then covered with staining solution (two volumes of ethanol and one volume of lactophenol were mixed and the final concentration of trypan blue was 1 mg/mL) in a six-

well microtiter plate and heated in a boiling water bath for 1 min. The plate was incubated at room temperature overnight. The staining solution was removed and the seedlings covered with destaining solution (staining solution without trypan blue) and incubated for ~2 to 6 h. The destaining solution was replaced and the samples incubated for an additional 12 h. The seedlings were covered with 70% glycerol for subsequent microscopy.

Analysis of SHMT Activity

Crude extracts for analysis of SHMT activity were prepared by grinding ~400 mg of leaf tissue in 300 μL of extraction buffer (50 mM phosphate buffer, 1 mM β-mercaptoethanol, and 2.5 mM EDTA), and the extracts were clarified by centrifugation at 4°C at 20,000*g* for 10 min. SHMT activity was tested by following the conversion of radioactive carbon from Ser to methylene THF. The assay was performed with 0.25 mM pyridoxal 5′ phosphate, 2 mM THF, 0.4 mM Ser [3-3H] Ser (33 Ci/mmol), and the crude extract in a final volume of 100 μL. Enzyme assays were performed at 37°C for 20 min. Then, 25 μL of the reaction mixture was streaked onto Whatman DE.81 paper. After drying the filter, unreacted Ser was removed by washing the filter three times with 20 mL of water for 20 min each. The radioactivity associated with methylene THF was measured by liquid scintillation counting.

Accession Numbers

Sequence data from this article can be found in the Arabidopsis Genome Initiative or GenBank/EMBL databases under the following accession numbers: At4g24560 (UBP16), At4g37930 (SHM1), and At4g13930 (SHM4).

Supplemental Data

The following materials are available in the online version of this article.

Supplemental Figure 1. Complementation of *ubp16* Restores Wild-Type—Like Tolerance to Salt.

Supplemental Figure 2. *UBP17* Is Not Involved the Response of *Arabidopsis* to Salt.

Supplemental Figure 3. Sensitivity of the *ubp16* Mutant to Alkali Metal Ions Is Specific for Na^+ and Li^+.

Supplemental Figure 4. *UBP16* Is Expressed in All Tissues in *Arabidopsis*.

Supplemental Figure 5. *UBP16* Expression Is Restored in Complemented Lines.

Supplemental Figure 6. The *ubp16* Mutant Phenocopies the Wild-Type Response to Low K^+.

Supplemental Figure 7. UBP16 Interacts with SHM1 and SHM4 but Not with SOS2 and SCaBP8 in Yeast.

Supplemental Figure 8. SHM4 Is Not Involved the Response of *Arabidopsis* to Salt.

Supplemental Figure 9. SHM1 Positively Modulates PM Na^+/H^+ Antiport Activity in *Arabidopsis*.

Supplemental Table 1. Primers Used for Plasmid Construction.

Supplemental Table 2. Primers Used for Real-Time PCR or RT-PCR Analysis.

Supplemental Data Set 1. Sequence Alignment of the 27 Members of the At-UBP Family.

ACKNOWLEDGMENTS

We thank the Arabidopsis Biological Resource Center for the T-DNA insertion lines. This work was supported by China National Funds for Distinguished Young Scientists (Grant 31025003 to Y.G.), the National Basic Research Program of China (Grant 2012CB114200 to Y.G.), the Foundation for Innovative Research Group of National Natural Science Foundation of China (Grant 31121002), and NSFC international collaborative research project (Grant 31210103903 to Y.G.).

AUTHOR CONTRIBUTIONS

H.Z. and J.Z. performed the research. H.Z., J.Z., and Y.G. designed the research and analyzed the data. Y.Y., C.C., Y.L., X.J., L.C., and X.L. performed the research on analysis of Na^+ and low K^+ sensitivity and Na^+/H^+ antiport activity. H.Z., J.Z., Y.G., X.W.D., and K.S.S. contributed to the discussion and wrote the article.

Received October 16, 2012; revised October 31, 2012; accepted November 20, 2012; published December 11, 2012.

REFERENCES

Allakhverdiev, S.I., Kinoshita, M., Inaba, M., Suzuki, I., and Murata, N. (2001). Unsaturated fatty acids in membrane lipids protect the photosynthetic machinery against salt-induced damage in *Synechococcus*. Plant Physiol. **125:** 1842–1853.

Amerik, A.Y., and Hochstrasser, M. (2004). Mechanism and function of deubiquitinating enzymes. Biochim. Biophys. Acta **1695:** 189–207.

An, R., Chen, Q.-J., Chai, M.-F., Lu, P.-L., Su, Z., Qin, Z.-X., Chen, J., and Wang, X.-C. (2007). AtNHX8, a member of the monovalent cation: proton antiporter-1 family in *Arabidopsis thaliana*, encodes a putative Li^+/H^+ antiporter. Plant J. **49:** 718–728.

Apse, M.P., Aharon, G.S., Snedden, W.A., and Blumwald, E. (1999). Salt tolerance conferred by overexpression of a vacuolar Na^+/H^+ antiport in *Arabidopsis*. Science **285:** 1256–1258.

Apse, M.P., Sottosanto, J.B., and Blumwald, E. (2003). Vacuolar cation/H^+ exchange, ion homeostasis, and leaf development are altered in a T-DNA insertional mutant of AtNHX1, the *Arabidopsis* vacuolar Na^+/H^+ antiporter. Plant J. **36:** 229–239.

Assmann, S.M., and Haubrick, L.L. (1996). Transport proteins of the plant plasma membrane. Curr. Opin. Cell Biol. **8:** 458–467.

Barragán, V., Leidi, E.O., Andrés, Z., Rubio, L., De Luca, A., Fernández, J.A., Cubero, B., and Pardo, J.M. (2012). Ion exchangers NHX1 and NHX2 mediate active potassium uptake into vacuoles to regulate cell turgor and stomatal function in *Arabidopsis*. Plant Cell **24:** 1127–1142.

Bauwe, H., and Kolukisaoglu, U. (2003). Genetic manipulation of glycine decarboxylation. J. Exp. Bot. **54:** 1523–1535.

Berthomieu, P., et al. (2003). Functional analysis of AtHKT1 in *Arabidopsis* shows that Na(+) recirculation by the phloem is crucial for salt tolerance. EMBO J. **22:** 2004–2014.

Brett, C.L., Donowitz, M., and Rao, R. (2005). Evolutionary origins of eukaryotic sodium/proton exchangers. Am. J. Physiol. Cell Physiol. **288:** C223–C239.

Chaves, M.M., Flexas, J., and Pinheiro, C. (2009). Photosynthesis under drought and salt stress: Regulation mechanisms from whole plant to cell. Ann. Bot. (Lond.) **103:** 551–560.

Chung, J.-S., Zhu, J.-K., Bressan, R.A., Hasegawa, P.M., and Shi, H. (2008). Reactive oxygen species mediate Na^+-induced SOS1 mRNA stability in *Arabidopsis*. Plant J. **53:** 554–565.

Cui, F., Liu, L., Zhao, Q., Zhang, Z., Li, Q., Lin, B., Wu, Y., Tang, S., and Xie, Q. (2012). *Arabidopsis* ubiquitin conjugase UBC32 is an ERAD component that functions in brassinosteroid-mediated salt stress tolerance. Plant Cell **24:** 233–244.

Davenport, R.J., Muñoz-Mayor, A., Jha, D., Essah, P.A., Rus, A., and Tester, M. (2007). The Na^+ transporter AtHKT1;1 controls retrieval of Na^+ from the xylem in *Arabidopsis*. Plant Cell Environ. **30:** 497–507.

De Gara, L., Locato, V., Dipierro, S., and de Pinto, M.C. (2010). Redox homeostasis in plants. The challenge of living with endogenous oxygen production. Respir. Physiol. Neurobiol. **173**(suppl.)**:** S13–S19.

Doelling, J.H., Phillips, A.R., Soyler-Ogretim, G., Wise, J., Chandler, J., Callis, J., Otegui, M.S., and Vierstra, R.D. (2007). The ubiquitin-specific protease subfamily UBP3/UBP4 is essential for pollen development and transmission in *Arabidopsis*. Plant Physiol. **145:** 801–813.

Engel, N., Ewald, R., Gupta, K.J., Zrenner, R., Hagemann, M., and Bauwe, H. (2011). The presequence of *Arabidopsis* serine hydroxymethyltransferase SHM2 selectively prevents import into mesophyll mitochondria. Plant Physiol. **157:** 1711–1720.

Fuglsang, A.T., Guo, Y., Cuin, T.A., Qiu, Q., Song, C., Kristiansen, K.A., Bych, K., Schulz, A., Shabala, S., Schumaker, K.S., Palmgren, M.G., and Zhu, J.-K. (2007). *Arabidopsis* protein kinase PKS5 inhibits the plasma membrane H^+ -ATPase by preventing interaction with 14-3-3 protein. Plant Cell **19:** 1617–1634.

Gaxiola, R.A., Li, J., Undurraga, S., Dang, L.M., Allen, G.J., Alper, S. L., and Fink, G.R. (2001). Drought- and salt-tolerant plants result from overexpression of the AVP1 H^+-pump. Proc. Natl. Acad. Sci. USA **98:** 11444–11449.

Geller, A.M., and Kotb, M.Y. (1989). A binding assay for serine hydroxymethyltransferase. Anal. Biochem. **180:** 120–125.

Haglund, K., and Dikic, I. (2005). Ubiquitylation and cell signaling. EMBO J. **24:** 3353–3359.

Hasegawa, P.M., Bressan, R.A., Zhu, J.-K., and Bohnert, H.J. (2000). Plant cellular and molecular responses to high salinity. Annu. Rev. Plant Physiol. Plant Mol. Biol. **51:** 463–499.

Hochstrasser, M. (1996). Ubiquitin-dependent protein degradation. Annu. Rev. Genet. **30:** 405–439.

Hoshida, H., Tanaka, Y., Hibino, T., Hayashi, Y., Tanaka, A., Takabe, T., and Takabe, T. (2000). Enhanced tolerance to salt stress in transgenic rice that overexpresses chloroplast glutamine synthetase. Plant Mol. Biol. **43:** 103–111.

Jamai, A., Salomé, P.A., Schilling, S.H., Weber, A.P.M., and McClung, C. R. (2009). *Arabidopsis* photorespiratory serine hydroxymethyltransferase activity requires the mitochondrial accumulation of ferredoxin-dependent glutamate synthase. Plant Cell **21:** 595–606.

Katiyar-Agarwal, S., Zhu, J., Kim, K., Agarwal, M., Fu, X., Huang, A., and Zhu, J.-K. (2006). The plasma membrane Na^+/H^+ antiporter SOS1 interacts with RCD1 and functions in oxidative stress tolerance in *Arabidopsis*. Proc. Natl. Acad. Sci. USA **103:** 18816–18821.

Kim, B.-G., Waadt, R., Cheong, Y.H., Pandey, G.K., Dominguez-Solis, J.R., Schültke, S., Lee, S.C., Kudla, J., and Luan, S. (2007). The calcium sensor CBL10 mediates salt tolerance by regulating ion homeostasis in *Arabidopsis*. Plant J. **52:** 473–484.

Kumar, S., Tamura, K., and Nei, M. (2004). MEGA3: Integrated software for Molecular Evolutionary Genetics Analysis and sequence alignment. Brief. Bioinform. **5:** 150–163.

Lakshmi, A., Ramanjulu, S., Veeranjaneyulu, K., and Sudhakar, C. (1996). Effect of NaCl on photosynthesis parameters in two cultivars of mulberry. Photosynthetica **32:** 285–289.

Li, W.-F., Perry, P.J., Prafulla, N.N., and Schmidt, W. (2010). Ubiquitin-specific protease 14 (UBP14) is involved in root responses to phosphate deficiency in *Arabidopsis*. Mol. Plant **3:** 212–223.

Lin, H., Yang, Y., Quan, R., Mendoza, I., Wu, Y., Du, W., Zhao, S., Schumaker, K.S., Pardo, J.M., and Guo, Y. (2009). Phosphorylation of SOS3-LIKE CALCIUM BINDING PROTEIN8 by SOS2 protein kinase stabilizes their protein complex and regulates salt tolerance in *Arabidopsis*. Plant Cell **21:** 1607–1619.

Liu, L., Cui, F., Li, Q., Yin, B., Zhang, H., Lin, B., Wu, Y., Xia, R., Tang, S., and Xie, Q. (2011). The endoplasmic reticulum-associated degradation is necessary for plant salt tolerance. Cell Res. **21:** 957–969.

Liu, Y., Wang, F., Zhang, H., He, H., Ma, L., and Deng, X.W. (2008). Functional characterization of the *Arabidopsis* ubiquitin-specific protease gene family reveals specific role and redundancy of individual members in development. Plant J. **55:** 844–856.

Luo, M., Luo, M.-Z., Buzas, D., Finnegan, J., Helliwell, C., Dennis, E.S., Peacock, W.J., and Chaudhury, A. (2008). UBIQUITIN-SPECIFIC PROTEASE 26 is required for seed development and the repression of PHERES1 in *Arabidopsis*. Genetics **180:** 229–236.

Luo, X., Budihardjo, I., Zou, H., Slaughter, C., and Wang, X. (1998). Bid, a Bcl2 interacting protein, mediates cytochrome c release from mitochondria in response to activation of cell surface death receptors. Cell **94:** 481–490.

Mäser, P., et al. (2001). Phylogenetic relationships within cation transporter families of *Arabidopsis*. Plant Physiol. **126:** 1646–1667.

McClung, C.R., Hsu, M., Painter, J.E., Gagne, J.M., Karlsberg, S.D., and Salomé, P.A. (2000). Integrated temporal regulation of the photorespiratory pathway. Circadian regulation of two *Arabidopsis* genes encoding serine hydroxymethyltransferase. Plant Physiol. **123:** 381–392.

Misra, A.N., Sahu, S.M., Misra, M., Singh, P., Meera, I., Das, N., Kar, M., and Sahu, P. (1997). Sodium chloride induced changes in leaf growth, and pigment and protein contents in two rice cultivars. Biol. Plant. **39:** 257–262.

Moreno, J.I., Martín, R., and Castresana, C. (2005). *Arabidopsis* SHMT1, a serine hydroxymethyltransferase that functions in the photorespiratory pathway influences resistance to biotic and abiotic stress. Plant J. **41:** 451–463.

Munns, R., and Tester, M. (2008). Mechanisms of salinity tolerance. Annu. Rev. Plant Biol. **59:** 651–681.

Qi, Z., and Spalding, E.P. (2004). Protection of plasma membrane K^+ transport by the salt overly sensitive1 Na^+-H^+ antiporter during salinity stress. Plant Physiol. **136:** 2548–2555.

Qiu, Q.-S., Guo, Y., Dietrich, M.A., Schumaker, K.S., and Zhu, J.-K. (2002). Regulation of SOS1, a plasma membrane Na^+/H^+ exchanger in *Arabidopsis thaliana*, by SOS2 and SOS3. Proc. Natl. Acad. Sci. USA **99:** 8436–8441.

Quan, R., Lin, H., Mendoza, I., Zhang, Y., Cao, W., Yang, Y., Shang, M., Chen, S., Pardo, J.M., and Guo, Y. (2007). SCABP8/CBL10, a putative calcium sensor, interacts with the protein kinase SOS2 to protect *Arabidopsis* shoots from salt stress. Plant Cell **19:** 1415–1431.

Rus, A., Lee, B.H., Muñoz-Mayor, A., Sharkhuu, A., Miura, K., Zhu, J.-K., Bressan, R.A., and Hasegawa, P.M. (2004). AtHKT1 facilitates Na^+ homeostasis and K^+ nutrition *in planta*. Plant Physiol. **136:** 2500–2511.

Senn, M.E., Rubio, F., Bañuelos, M.A., and Rodríguez-Navarro, A. (2001). Comparative functional features of plant potassium HvHAK1 and HvHAK2 transporters. J. Biol. Chem. **276:** 44563–44569.

Serrano, R., Mulet, J.M., Rios, G., Marquez, J.A., Larrinoa, I.F.d., Leube, M.P., Mendizabal, I., Pascual-Ahuir, A., Proft, M., Ros, R., and Montesinos, C. (1999). A glimpse of the mechanisms of ion homeostasis during salt stress. J. Exp. Bot. **50:** 1023–1036.

Sheen, J. (2001). Signal transduction in maize and *Arabidopsis* mesophyll protoplasts. Plant Physiol. **127:** 1466–1475.

Shi, H., Ishitani, M., Kim, C., and Zhu, J.-K. (2000). The *Arabidopsis thaliana* salt tolerance gene SOS1 encodes a putative Na^+/H^+ antiporter. Proc. Natl. Acad. Sci. USA **97:** 6896–6901.

Shi, H., Quintero, F.J., Pardo, J.M., and Zhu, J.-K. (2002). The putative plasma membrane Na^+/H^+ antiporter SOS1 controls long-distance Na^+ transport in plants. Plant Cell **14:** 465–477.

Somerville, C.R., and Ogren, W.L. (1981). Photorespiration-deficient mutants of *Arabidopsis thaliana* lacking mitochondrial serine transhydroxymethylase activity. Plant Physiol. **67:** 666–671.

Sridhar, V.V., Kapoor, A., Zhang, K., Zhu, J., Zhou, T., Hasegawa, P.M., Bressan, R.A., and Zhu, J.-K. (2007). Control of DNA methylation and heterochromatic silencing by histone H2B deubiquitination. Nature **447:** 735–738.

Thompson, J.D., Higgins, D.G., and Gibson, T.J. (1994). CLUSTAL W: Improving the sensitivity of progressive multiple sequence alignment through sequence weighting, position-specific gap penalties and weight matrix choice. Nucleic Acids Res. **22:** 4673–4680.

Timm, S., Nunes-Nesi, A., Pärnik, T., Morgenthal, K., Wienkoop, S., Keerberg, O., Weckwerth, W., Kleczkowski, L.A., Fernie, A.R., and Bauwe, H. (2008). A cytosolic pathway for the conversion of hydroxypyruvate to glycerate during photorespiration in *Arabidopsis*. Plant Cell **20:** 2848–2859.

Torres, M.A. (2010). ROS in biotic interactions. Physiol. Plant. **138:** 414–429.

Vidal, G., Ribas-Carbo, M., Garmier, M., Dubertret, G., Rasmusson, A.G., Mathieu, C., Foyer, C.H., and De Paepe, R. (2007). Lack of respiratory chain complex I impairs alternative oxidase engagement and modulates redox signaling during elicitor-induced cell death in tobacco. Plant Cell **19:** 640–655.

Voll, L.M., Jamai, A., Renné, P., Voll, H., McClung, C.R., and Weber, A.P.M. (2006). The photorespiratory *Arabidopsis shm1* mutant is deficient in SHM1. Plant Physiol. **140:** 59–66.

Wang, F., Zhu, D., Huang, X., Li, S., Gong, Y., Yao, Q., Fu, X., Fan, L.-M., and Deng, X.W. (2009). Biochemical insights on degradation of *Arabidopsis* DELLA proteins gained from a cell-free assay system. Plant Cell **21:** 2378–2390.

Welchman, R.L., Gordon, C., and Mayer, R.J. (2005). Ubiquitin and ubiquitin-like proteins as multifunctional signals. Nat. Rev. Mol. Cell Biol. **6:** 599–609.

Wilkinson, K.D. (2000). Ubiquitination and deubiquitination: Targeting of proteins for degradation by the proteasome. Semin. Cell Dev. Biol. **11:** 141–148.

Wing, S.S. (2003). Deubiquitinating enzymes—The importance of driving in reverse along the ubiquitin-proteasome pathway. Int. J. Biochem. Cell Biol. **35:** 590–605.

Xu, J., Li, H.-D., Chen, L.-Q., Wang, Y., Liu, L.-L., He, L., and Wu, W.-H. (2006). A protein kinase, interacting with two calcineurin B-like proteins, regulates K^+ transporter AKT1 in *Arabidopsis*. Cell **125:** 1347–1360.

Yang, Y., Qin, Y., Xie, C., Zhao, F., Zhao, J., Liu, D., Chen, S., Fuglsang, A.T., Palmgren, M.G., Schumaker, K.S., Deng, X.W., and Guo, Y. (2010). The *Arabidopsis* chaperone J3 regulates the plasma membrane H^+-ATPase through interaction with the PKS5 kinase. Plant Cell **22:** 1313–1332.

Yokoi, S., Quintero, F.J., Cubero, B., Ruiz, M.T., Bressan, R.A., Hasegawa, P.M., and Pardo, J.M. (2002). Differential expression and function of *Arabidopsis thaliana* NHX Na^+/H^+ antiporters in the salt stress response. Plant J. **30:** 529–539.

Zhu, J.-K. (2003). Regulation of ion homeostasis under salt stress. Curr. Opin. Plant Biol. **6:** 441–445.